Electronic Research Archive

https://www.aimspress.com/journal/era

ERA, 33(9): 5426–5456.
DOI: 10.3934/era.2025243
Received: 26 June 2025
Revised: 07 August 2025
Accepted: 14 August 2025
Published: 15 September 2025

Research article

Analyzing diffusive vegetation-sand model: Instability, bifurcation, and pattern formation

Gaihui Guo[1,*], Xinyue Zhang[1], Jichun Li[1,2] and Tingting Wei[1]

[1] School of Mathematics and Data Science, Shaanxi University of Science and Technology, Xi'an, Shaanxi 710021, China

[2] School of Mathematics and Statistics, Xidian University, Xi'an, Shaanxi 710126, China

* **Correspondence:** Email: guogaihui@sust.edu.cn.

Abstract: In this study, we explored a diffusive vegetation-sand model with Neumann boundary conditions, investigating the role of Turing instability in vegetation pattern formation. A priori estimates for steady-state solutions were established using the maximum principle and Poincaré inequality. Bifurcation analysis was performed for simple and double eigenvalue cases. By employing bifurcation theory, a local bifurcation was extended globally, and the direction of bifurcation was characterized. Double eigenvalue cases were analyzed through spatial decomposition and the implicit function theorem. Finally, numerical simulations validated and complemented the theoretical results.

Keywords: vegetation-sand model; turing instability; steady-state bifurcation; vegetation pattern; double eigenvalue

1. Introduction

Vegetation patterns induced by aeolian sand movement represent a typical form of spatial organization in arid and semi-arid regions. These patterns often appear as striking landscapes near desert margins [1]. In recent years, ecosystems have been increasingly disrupted by natural forces and anthropogenic activities, intensifying the process of desertification. Understanding the interaction between vegetation and sand is therefore of significant and ecological importance.

As early as 1962, it was suggested that wind might initiate the formation of banded vegetation in Jordan [2, 3]. Subsequent studies emphasized the crucial role of wind-driven sand accumulation around plants in vegetation growth cycles [4–6]. Fine aeolian sand particles deposited on leaf and stem surfaces hinder vegetation photosynthesis, reduce soil moisture, and suppress plant growth. Beyond the vegetation's location, aeolian sand across the surrounding and broader study area impedes foliage development. During transport, the sand abrades stems and leaves, damaging tissues and

reducing vegetation productivity. This wind-driven sand burial process constitutes a negative feedback mechanism: Increasing vegetation coverage enhances sand deposition, which in turn suppresses vegetation growth.

Given the above ecological importance of sand-related effects, it is necessary to construct mathematical models that explicitly describe vegetation-sand interactions. Although vegetation model research has primarily emphasized vegetation-water interactions, vegetation-sand dynamics remain underexplored. Rainfall variability is considered a driver of transitions among bare soil, vegetation pattern, and homogeneous vegetation states [7–9]. Extensions of vegetation models have been proposed to capture more realistic ecological processes, such as inertial effects, autotoxicity, cross-diffusion, and nonlocal interactions. These studies further demonstrate the value of mathematical tools in exploring vegetation-water and vegetation-sand dynamics under complex environmental feedbacks [10, 11].

A pioneering model of vegetation patterns was proposed by Klausmeier [12] in 1999, which predicted the formation and uphill migration of vegetation patterns along slopes. In 2013, van der Stelt et al. [13] extended the Klausmeier model by introducing water diffusion and obtained the GKGS model. In addition, many researchers have addressed vegetation pattern formation through ecohydrological mechanisms. In particular, previous studies developed models that reveal the mechanisms underlying vegetation pattern emergence under varying rainfall conditions, including positive feedbacks, scale-dependent dispersal, and localized disturbances [14–16]. More recently, studies explored vegetation-water interactions with cross-diffusion and delay effects, uncovering complex bifurcation structures and spatiotemporal dynamics [17].

Zhang et al. [18] proposed a model involving vegetation cover and aeolian sand accumulation height, as follows,

$$\begin{cases} \dfrac{\partial S}{\partial T} = K_0 + MV\left(1 - \dfrac{V}{V_0}\right) - NS - A_1\dfrac{\partial S}{\partial X} + D_1\left(\dfrac{\partial^2 S}{\partial X^2} + \dfrac{\partial^2 S}{\partial Y^2}\right), \\ \dfrac{\partial V}{\partial T} = HV\left(1 - \dfrac{V}{V_m}\right) - PS\dfrac{V}{C+V} - A_2\dfrac{\partial V}{\partial X} + D_2\left(\dfrac{\partial^2 V}{\partial X^2} + \dfrac{\partial^2 V}{\partial Y^2}\right), \end{cases} \tag{1.1}$$

where $\frac{\partial S}{\partial T}$ and $\frac{\partial V}{\partial T}$ denote the accumulation rate of sand and vegetation growth rate, respectively. $K_0 + MV(1 - \frac{V}{V_0}) - NS$ describes sand deposition by vegetation. $A_1\frac{\partial S}{\partial X}$ and $A_2\frac{\partial V}{\partial X}$ represent advection and dispersal driven by prevailing wind. $HV(1 - \frac{V}{V_m})$ models vegetation growth, and $PS\frac{V}{C+V}$ accounts for sand-induced vegetation loss. The terms $D_1(\frac{\partial^2 S}{\partial X^2} + \frac{\partial^2 S}{\partial Y^2})$ and $D_2(\frac{\partial^2 V}{\partial X^2} + \frac{\partial^2 V}{\partial Y^2})$ describe isotropic sand diffusion and vegetation dispersal.

System (1.1) explores how wind-sand dynamics influence vegetation spatial distribution under windy conditions. Prevailing wind alters vegetation cover and sand transport via advection, while other wind effects are incorporated through diffusion. Excess aeolian sand may lead to vegetation burial. In many regions, prevailing winds are not pronounced, leading to the following model

$$\begin{cases} \dfrac{\partial S}{\partial T} = K_0 + MV\left(1 - \dfrac{V}{V_0}\right) - NS + D_1\left(\dfrac{\partial^2 S}{\partial X^2} + \dfrac{\partial^2 S}{\partial Y^2}\right), \\ \dfrac{\partial V}{\partial T} = HV\left(1 - \dfrac{V}{V_m}\right) - PS\dfrac{V}{C+V} + D_2\left(\dfrac{\partial^2 V}{\partial X^2} + \dfrac{\partial^2 V}{\partial Y^2}\right). \end{cases} \tag{1.2}$$

Zhang et al. [18] noted that the aggregation effect of vegetation on sand weakens as biomass increases. In contrast, we focuses on the mechanism underlying the aggregation effect introduced by

the linear action term. The system (1.2) is reformulated as follows,

$$\begin{cases} \dfrac{\partial S}{\partial T} = K_0 + MV - NS + D_1\Delta S, \\ \dfrac{\partial V}{\partial T} = HV\left(1 - \dfrac{V}{V_m}\right) - PS\dfrac{V}{C+V} + D_2\Delta V. \end{cases} \tag{1.3}$$

For ease of analysis, let

$$s = \frac{N}{K_0}S, \quad v = \frac{M}{K_0}V, \quad t = NT, \quad h = \frac{H}{N}, \quad v_m = \frac{MV_m}{K_0}, \quad p = \frac{PK_0}{CN^2},$$

$$c = \frac{K_0}{CM}, \quad D_1 = d_1, \quad D_2 = d_2, \quad x = \sqrt{N}X, \quad y = \sqrt{N}Y.$$

Hence, the resulting dimensionless system (1.3) is given below

$$\begin{cases} \dfrac{\partial s(x,t)}{\partial t} - d_1\Delta s(x,t) = 1 + v - s, & x \in \Omega,\ t > 0, \\ \dfrac{\partial v(x,t)}{\partial t} - d_2\Delta v(x,t) = hv\left(1 - \dfrac{v}{v_m}\right) - ps\dfrac{v}{1+cv}, & x \in \Omega,\ t > 0, \\ \dfrac{\partial s(x,t)}{\partial \mathrm{n}} = \dfrac{\partial v(x,t)}{\partial \mathrm{n}} = 0, & x \in \partial\Omega,\ t > 0, \\ s(x,0) = s_0(x) \geq 0,\ \not\equiv 0, \quad v(x,0) = v_0(x) \geq 0,\ \not\equiv 0, & x \in \overline{\Omega}, \end{cases} \tag{1.4}$$

where s and v denote the sand accumulation height and vegetation coverage, respectively. h denotes vegetation's intrinsic growth rate, and v_m its maximum potential. p represents the destructive effect of sand burial, while c denotes the half-saturation constant for sand capacity. d_1 and d_2 represent the diffusivity ratio of vegetation to sand. Δ denotes the standard Laplace operator. Ω is a bounded domain in $\mathbb{R}^n$ ($n \geq 1$) with smooth boundary $\partial\Omega$, and n is the unit outward normal on $\partial\Omega$. The non-dimensionalization preserves Neumann boundary conditions. Nonnegative initial data ensure positivity of the solution, and $s_0(x)$ and $v_0(x)$ do not influence subsequent analysis.

The vegetation-sand model has attracted considerable attention. For model (1.2), Zhang et al. [1] incorporated the effects of sand movement into vegetation diffusion via a cross-diffusion term. An improved model was subsequently proposed to investigate how cross-diffusion influences vegetation pattern formation and transition, supported by Turing bifurcation and amplitude analyses. Maimaiti et al. [19] developed a fractional-order vegetation-sand model to study the spatiotemporal dynamics of vegetation patterns. Through stability analysis and numerical simulations, they explored the effects of environmental conditions and the role of fractional derivatives in vegetation-sand interactions, providing insights into ecological restoration and land management strategies. Furthermore, Zhang et al. [20] investigated the self-organized formation of vegetation patterns using the vegetation-sand model. They simulated the formation of vegetation patterns under different bifurcation scenarios, calculating the Shannon entropy and contagion index to explore the role of these statistical indicators in the pattern formation process.

Many scholars have made substantial progress in the stability and bifurcation analysis of vegetation models. Zhang et al. [21] revealed the impact of soil-water diffusion on vegetation pattern through steady-state bifurcation. Wang et al. [22] analyzed a reaction-diffusion system for water-plant

interaction based on the Klausmeier model, where non-constant steady-state and large-amplitude spatial pattern were identified through bifurcation and shadow system techniques. Guo and Wang [23] investigated a vegetation-water model with diffusion, analyzing stability, Turing instability, and bifurcations at simple and double eigenvalues, supported by numerical simulations. Wang et al. [24] examined vegetation pattern formation in a water-biomass model, identifying conditions for Turing instability and the emergence of spatial patterns under different parameters. Grifó et al. [25] addressed the formation of rhombic and hexagonal Turing patterns in bidimensional hyperbolic reaction-transport systems in the context of the Klausmeier vegetation model. In addition to vegetation models, other models involving resource competition, diffusion, and bifurcation analysis have been explored. Wu et al. [26, 27] studied chemostat models of species competition for resources and steady-state conditions for multistability. Ma and Yang [28] analyzed a modified Leslie-Gower model with nonlocal competition, while Zhu and Yang [29] investigated bifurcation with nonlocal competition and fear effects, showing that Hopf, Turing, and Hopf-Hopf bifurcations generate spatiotemporal dynamics.

Inspired by the preceding studies, we analyze the steady-state solutions of system (1.4). The corresponding model is given by

$$\begin{cases} -d_1\Delta s(x,t) = 1+v-s, & x\in\Omega,\ t>0,\\ -d_2\Delta v(x,t) = hv\left(1-\dfrac{v}{v_m}\right)-ps\dfrac{v}{1+cv}, & x\in\Omega,\ t>0,\\ \partial_{\mathrm{n}} s=\partial_{\mathrm{n}} v=0, & x\in\partial\Omega,\ t>0. \end{cases} \tag{1.5}$$

By taking d_1 as the bifurcation parameter, we analyze steady-state bifurcations arising from the positive equilibrium. Compared with [1, 5, 27], the primary contribution of this work lies in the bifurcation analysis at both simple and double eigenvalues, including the extension from local to global bifurcations and the determination of bifurcation direction.

The structure of the paper is as follows. In Section 2, we examine the stability of the positive equilibrium and the influence of diffusion on Turing instability. In Section 3, we provide a priori estimates for positive steady-state solutions. In Section 4, we present the bifurcation analysis, covering local and global bifurcations as well as bifurcation direction. In Section 5, we offer numerical simulations to validate and complement the theoretical findings.

2. Turing instability analysis

To obtain the conditions to ensure the discovery of Turing instability for the reaction-diffusion system (1.4), we investigate the stability of the positive equilibrium without diffusion for the following system

$$\begin{cases} \dfrac{\mathrm{d}s}{\mathrm{d}t} = 1+v-s, & t>0,\\ \dfrac{\mathrm{d}v}{\mathrm{d}t} = hv\left(1-\dfrac{v}{v_m}\right)-ps\dfrac{v}{1+cv}, & t>0. \end{cases} \tag{2.1}$$

For $v = 0$ and $s = 1$, system (2.1) admits a unique bare sand equilibrium $Q_0 = (1, 0)$. In contrast, for $v \neq 0$, we have

$$-\frac{ch}{v_m}v^2 + \left(ch - p - \frac{h}{v_m}\right)v + h - p = 0. \tag{2.2}$$

Let

$$A = -\frac{ch}{v_m} < 0, \quad B = ch - p - \frac{h}{v_m}, \quad C = h - p.$$

Equilibria of system (2.1) are determined by parameter relations in the above constant equation, as detailed in the following cases:

(i) When the parameters satisfy $B^2 - 4AC > 0$ and $B > \sqrt{B^2 - 4AC}$, Eq (2.2) has two positive roots

$$v_{11} = \frac{-B + \sqrt{B^2 - 4AC}}{2A}, \quad v_{12} = \frac{-B - \sqrt{B^2 - 4AC}}{2A}.$$

Therefore, $s_{11} = 1 + v_{11}$ and $s_{12} = 1 + v_{12}$, implying that system (2.1) admits two uniformly vegetated equilibrium points: $Q_{11} = (s_{11}, v_{11})$, $Q_{12} = (s_{12}, v_{12})$.

(ii) When $B^2 - 4AC = 0$ and $B > 0$, Eq (2.2) admits a unique positive root $v_2 = -\frac{B}{2A}$, with $s_2 = 1 + v_2$. Hence, system (2.1) has an equilibrium point $Q_2 = (s_2, v_2)$.

(iii) When $B^2 - 4AC < 0$, Eq (2.2) has no real roots, implying that system (2.1) possesses no equilibrium.

To analyze the stability of the equilibrium point, we evaluate the Jacobian matrix of the system at the equilibrium point $Q^* = (s_*, v_*)$, given by

$$J = \begin{pmatrix} -1 & 1 \\ -\dfrac{pv_*}{1 + cv_*} & h - \dfrac{2hv_*}{v_m} - \dfrac{ps_*}{(1 + cv_*)^2} \end{pmatrix} = \begin{pmatrix} -1 & 1 \\ -N & H \end{pmatrix}.$$

Let $H = h - \dfrac{2hv_*}{v_m} - \dfrac{ps_*}{(1 + cv_*)^2}$ and $N = \dfrac{pv_*}{1 + cv_*}$, then the corresponding characteristic equation is

$$\mu^2 - \mathrm{Tr}J\mu + \mathrm{Det}J = 0,$$

where

$$\mathrm{Tr}J = H - 1, \quad \mathrm{Det}J = N - H.$$

Suppose that $h_0 = \left(1 + \dfrac{ps_*}{(1 + cv_*)^2}\right) \cdot \dfrac{v_m}{v_m - 2v_*}$ and $H < N$. For system (2.1), the following results are true.

(i) Suppose $h < h_0$. Then the trace satisfies $\mathrm{Tr}J = H - 1 < 0$, and the determinant $\mathrm{Det}J = N - H > 0$, indicating that the equilibrium (s_*, v_*) is locally asymptotically stable.

(ii) Assume that $h > h_0$. Then, $\mathrm{Tr}J > 0$, $\mathrm{Det}J > 0$, and the equilibrium (s_*, v_*) becomes unstable.

(iii) Assume that $h = h_0$. Then, the Jacobian matrix J has a pair of purely imaginary eigenvalues and the transversality condition is satisfied, since $\dfrac{d}{dh}\mathrm{Re}(\lambda)\Big|_{h=h_0} = \dfrac{1}{2}\left(1 - \dfrac{2v_*}{v_m}\right) \neq 0$. Therefore, system (2.1) undergoes a Hopf bifurcation at the equilibrium (s_*, v_*) when $h = h_0$. The following discussions are conducted under the conditions that $H < 1$ and $H < N$ are satisfied.

Let

$$0 = \lambda_0 < \lambda_1 < \cdots < \lambda_i < \cdots$$

be the eigenvalues of the operator $-\Delta$ with Neumann boundary conditions on Ω, each with multiplicity m_i $(i = 0, 1, 2, \ldots)$. Let $\{\phi_{ij}\}_{1\le j\le m_i}$ denote the corresponding normalized eigenfunctions, and define $\phi_i = \phi_{i1}$. Then, $\{\phi_{ij}\}_{i\ge 0,\, 1\le j\le m_i}$ forms a complete orthonormal basis of $L^2(\Omega)$.

By substituting $(1+\beta, \beta)$ into the expression of H, we obtain the inequality $d_2\lambda_1 < h - \dfrac{2h\beta}{v_m} - \dfrac{p(1+\beta)}{(1+c\beta)^2}$. Let i_0 denote the largest positive integer, satisfying

$$d_2\lambda_i < h - \frac{2h\beta}{v_m} - \frac{p(1+\beta)}{(1+c\beta)^2} \quad \text{for} \quad 1 \le i \le i_0.$$

The threshold $\widetilde{d_1} = \min_{1\le i\le i_0} d_{1,i}$ ensures stability across all unstable spatial modes, where each $d_{1,i}$ solves $N_i = 0$ for the i-th mode. This minimum criterion guarantees suppression of the most sensitive perturbation mode. Let

$$\widetilde{d_1} = \min_{1\le i\le i_0} d_{1,i}, \tag{2.3}$$

where

$$d_{1,i} = \frac{d_2\lambda_i + (-h + \dfrac{2h\beta}{v_m} + \dfrac{pc\beta^2 + 2p\beta + p}{(1+c\beta)^2})}{\lambda_i(h - \dfrac{2h\beta}{v_m} - \dfrac{p(1+\beta)}{(1+c\beta)^2} - d_2\lambda_i)}.$$

Thus, (s_*, v_*) is locally asymptotically stable for (1.4) as presented in the following theorem.

Theorem 2.1. *Assume $H < 1$ and $H < N$ hold. Then, we have*

(i) *When $d_2\lambda_1 \ge h - \dfrac{2h\beta}{v_m} - \dfrac{p(1+\beta)}{(1+c\beta)^2}$, the equilibrium (s_*, v_*) is stable under any $d_1 > 0$ for (1.4).*

(ii) *Let $d_2\lambda_1 < h - \dfrac{2h\beta}{v_m} - \dfrac{p(1+\beta)}{(1+c\beta)^2}$. If $d_1 < \widetilde{d_1}$, the equilibrium (s_*, v_*) is stable for (1.4); If $d_1 > \widetilde{d_1}$, the equilibrium (s_*, v_*) becomes unstable for (1.4).*

Proof. To linearize system (1.4) at (s_*, v_*), we have

$$\begin{pmatrix} s_t \\ v_t \end{pmatrix} = L\begin{pmatrix} s \\ v \end{pmatrix} = \begin{pmatrix} -1 + d_1\Delta & 1 \\ -\dfrac{p\beta}{1+c\beta} & h - \dfrac{2h\beta}{v_m} - \dfrac{p(1+\beta)}{(1+c\beta)^2} + d_2\Delta \end{pmatrix}\begin{pmatrix} s \\ v \end{pmatrix}.$$

Let (ψ_1, ψ_2) be the eigenfunction of L corresponding to the eigenvalue μ. We have

$$\begin{pmatrix} -1 + d_1\Delta & 1 \\ -\dfrac{p\beta}{1+c\beta} & h - \dfrac{2h\beta}{v_m} - \dfrac{p(1+\beta)}{(1+c\beta)^2} + d_2\Delta \end{pmatrix}\begin{pmatrix} \psi_1 \\ \psi_2 \end{pmatrix} = \mu\begin{pmatrix} \psi_1 \\ \psi_2 \end{pmatrix}.$$

If we set

$$\psi_1 = \sum_{0\le i\le\infty, 1\le j\le\infty} a_{ij}\phi_{ij}, \quad \psi_2 = \sum_{0\le i\le\infty, 1\le j\le\infty} b_{ij}\phi_{ij},$$

calculated as

$$\sum_{0\le i\le\infty,1\le j\le\infty}\begin{pmatrix} -1-d_1\lambda_i-\mu & 1 \\ -\dfrac{p\beta}{1+c\beta} & h-\dfrac{2h\beta}{v_m}-\dfrac{p(1+\beta)}{(1+c\beta)^2}-d_2\lambda-\mu \end{pmatrix}\begin{pmatrix} a_{ij} \\ b_{ij} \end{pmatrix}\phi_{ij}=0.$$

μ is an eigenvalue of L if and only if

$$\mu^2-M_i\mu+N_i=0 \quad (i=0,1,2,\cdots), \tag{2.4}$$

where

$$M_i=h-\frac{2h\beta}{v_m}-\frac{p(1+\beta)}{(1+c\beta)^2}-1-(d_1+d_2)\lambda_i,$$

$$N_i=d_1d_2\lambda_i^2+\left(d_1\left(-h+\frac{2h\beta}{v_m}+\frac{p(1+\beta)}{(1+c\beta)^2}\right)+d_2\right)\lambda_i+\left(-h+\frac{2h\beta}{v_m}+\frac{pc\beta^2+2p\beta+p}{(1+c\beta)^2}\right).$$

Since $H<1$ and $H<N$, we have $M_i<0$ for all $i\ge 0$. We see that $N_0>0$. Thus, we focus on the sign of M_i $(i\ge 1)$.

If $d_2\lambda_1 \ge h-\dfrac{2h\beta}{v_m}-\dfrac{p(1+\beta)}{(1+c\beta)^2}$, then $N_i = d_1\lambda_i\left(d_2\lambda_i-h+\dfrac{2h\beta}{v_m}+\dfrac{p(1+\beta)}{(1+c\beta)^2}\right)+d_2\lambda_i+\left(-h+\dfrac{2h\beta}{v_m}+\dfrac{pc\beta^2+2p\beta+p}{(1+c\beta)^2}\right)>0$ for $i\ge 1$, implying $Re(\mu)<0$ for all eigenvalues μ of L, and that (s_*,v_*) is locally asymptotically stable for (1.4).

If $d_2\lambda_1<h-\dfrac{2h\beta}{v_m}-\dfrac{p(1+\beta)}{(1+c\beta)^2}$ and $0<d_1<\tilde{d}_1$, then $d_2\lambda_i<h-\dfrac{2h\beta}{v_m}-\dfrac{p(1+\beta)}{(1+c\beta)^2}$ and $0<d_1<\tilde{d}_{1,i}$ for $1\le i\le i_0$, leading to $N_i>0$ in this range. For $i>i_0$, since $d_2\lambda_1\ge h-\dfrac{2h\beta}{v_m}-\dfrac{p(1+\beta)}{(1+c\beta)^2}$ and $0<d_1<\tilde{d}_1$, we also obtain $N_i>0$. Therefore, (s_*,v_*) remains locally asymptotically stable in system (1.4).

If $d_2\lambda_1<h-\dfrac{2h\beta}{v_m}-\dfrac{p(1+\beta)}{(1+c\beta)^2}$ and $d_1>\tilde{d}_1$, let the minimum in (2.3) be attained at $j\in[1,i_0]$, which gives $d_1>d_{1,j}$, implying

$$N_i=d_1\lambda_i\left(d_2\lambda_i-h+\frac{2h\beta}{v_m}+\frac{p(1+\beta)}{(1+c\beta)^2}\right)+d_2\lambda_i+\left(-h+\frac{2h\beta}{v_m}+\frac{pc\beta^2+2p\beta+p}{(1+c\beta)^2}\right)<0.$$

Hence, (s_*,v_*) is unstable for (1.4).

3. A priori estimates

In this section, we derive a priori estimates for non-constant positive solutions to (1.5). We begin with the following lemma.

Lemma 3.1 ([30]). *Suppose* $q\in C\left(\overline{\Omega}\times\mathbb{R}\right)$.

(i) *Let* $s(x)\in C^2(\Omega)\cap C^1(\overline{\Omega})$ *satisfy*

$$\Delta s(x)+q\left(x,s(x)\right)\ge 0,\quad x\in\Omega,\quad \partial_v s\le 0,\quad x\in\partial\Omega.$$

If $s(x_0)=\max_{\overline{\Omega}}s(x)$, *then* $q\left(x_0,s(x_0)\right)\ge 0$.

(ii) *Let* $s(x)\in C^2(\Omega)\cap C^1(\overline{\Omega})$ *satisfy*

$$\Delta s(x) + q\,(x, s(x)) \le 0, \quad x \in \Omega, \quad \partial_v s \ge 0, \quad x \in \partial\Omega.$$

If $s(x_0) = \min_{\overline{\Omega}} s(x)$*, then* $q\,(x_0, s(x_0)) \le 0$*.*

Next, we establish a priori estimates for nonnegative solutions of (1.5).

Theorem 3.1. *Let* (s, v) *be any given positive solution of (1.5). We can get that there is a positive constant* $C_0 = C_0(d_2, h, v_m, p, c, \Omega)$ *that satisfies*

$$1 \le s \le 1 + v_m, \quad \frac{v_m(h-p)}{h} \le v \le v_m.$$

Proof. From the first equation for s of (1.5), it follows that

$$d_1\Delta s + 1 + v - s \ge 0.$$

Let $s(x_1) = \max\limits_{\bar{\Omega}} s(x)$. From Lemma 3.1, it follows that

$$s(x_1) \le 1 + v(x_1) \le 1 + \max_{\bar{\Omega}} v(x),$$

then

$$s(x_1) \le 1 + v(x_1) \le 1 + \max_{\bar{\Omega}} v(x). \tag{3.1}$$

It can be deduced from the second equation of v in (1.5) that

$$d_2\Delta v + hv\left(1 - \frac{v}{v_m}\right) - \frac{psv}{1+cv} \ge 0.$$

Let $v(x_2) = \max\limits_{\bar{\Omega}} v(x)$. From Lemma 3.1, we obtain

$$h\left(1 - \frac{v(x_2)}{v_m}\right) - \frac{ps(x_2)}{1+cv(x_2)} \ge 0.$$

Thus, we can get

$$h - \frac{ps(x_2)}{1+cv(x_2)} \ge \frac{hv(x_2)}{v_m},$$

so we have $v(x_2) \le v_m$ and combining with (3.1), we finally get $s(x_1) \le 1 + v_m$.

Let $s(x_3) = \min\limits_{\bar{\Omega}} s(x)$. Then, we get

$$1 + v(x_3) - s(x_3) \le 0.$$

Thus, $s(x_3) \ge 1$. Let $v(x_4) = \min\limits_{\bar{\Omega}} v(x)$. So we have

$$h\left(1 - \frac{v(x_4)}{v_m}\right) - \frac{ps(x_4)}{1+cv(x_4)} \le 0.$$

And we see that

$$h - ps(x_4) \le h - \frac{ps(x_4)}{1+cv(x_4)} \le \frac{hv(x_4)}{v_m}.$$

Thus, we get

$$[h - p\max_{\bar{\Omega}} s(x)]v_m \le (h - ps(x_4))v_m \le hv(x_4),$$

which implies

$$v(x_4) \ge \frac{v_m}{h}\left(h - p\max_{\bar{\Omega}} s(x)\right) \ge \frac{(h - p(1 + v_m))v_m}{h}.$$

The proof is complete.

4. The steady-state bifurcation

Assuming $\Omega = (0, \pi)$, we investigate the existence of non-constant positive solutions to system (1.5). Moreover, the results are applicable to higher-dimensional spatial domains.

Let d_1 be the bifurcation parameter. We aim to establish the existence of non-constant positive solutions bifurcating from (s_*, v_*) in the following elliptic system

$$\begin{cases} -d_1 s'' = 1 + v - s, & x \in (0, \pi), \\ -d_2 v'' = hv\left(1 - \dfrac{v}{v_m}\right) - ps\dfrac{v}{1 + cv}, & x \in (0, \pi), \\ s' = v' = 0, & x \in \{0, \pi\}. \end{cases} \tag{4.1}$$

To explore the structure and direction of the bifurcation branches, we shift the equilibrium (s_*, v_*) to the origin via the transformation

$$\widetilde{s} = s - s_*, \quad \widetilde{v} = v - v_*.$$

For simplicity, we continue to denote $\widetilde{s}$ and $\widetilde{v}$ by s and v, respectively. Under this translation, system (4.1) becomes

$$\begin{cases} -d_1 s'' = 1 + (v + v_*) - (s + s_*), & x \in (0, \pi), \\ -d_2 v'' = h(v + v_*)\left(1 - \dfrac{v + v_*}{v_m}\right) - p(s + s_*)\dfrac{v + v_*}{1 + c(v + v_*)}, & x \in (0, \pi), \\ s' = v' = 0, & x \in \{0, \pi\}. \end{cases} \tag{4.2}$$

4.1. Local steady-state bifurcation

In this subsection, we analyze the local steady-state bifurcation of system (4.2). Initially, bifurcations arising from simple eigenvalues are derived via the Crandall-Rabinowitz bifurcation theorem. Subsequently, utilizing space decomposition and the implicit function theorem, we address the case involving double eigenvalues.

We adopt the standard Sobolev space $W^{2,2}(0, \pi)$, consisting of functions whose derivatives up to second order are square integrable, endowed with the Sobolev norm. The Banach space $B^2(0, \pi)$ is taken as the space of twice continuously differentiable functions on $(0, \pi)$, equipped with the C^2-norm. These function spaces form the basis for the bifurcation operator framework.

Define

$$X = \left\{(s_*, v_*) \in W^{2,2}(0, \pi) \times W^{2,2}(0, \pi) : s' = v' = 0,\ x = 0, \pi\right\}, \quad Y = B^2(0, \pi) \times B^2(0, \pi),$$

and introduce the map $F : \mathbb{R}^+ \times X \to Y$ by

$$F(d_1, U) = \begin{pmatrix} d_1 s'' + 1 + (v + v_*) - (s + s_*) \\ d_2 v'' + h(v + v_*)\left(1 - \dfrac{v + v_*}{v_m}\right) - p(s + s_*)\dfrac{v + v_*}{1 + c(v + v_*)} \end{pmatrix}, \quad U = (s, v)^T.$$

The solutions to (2.4) correspond precisely to the zeros of F, and evidently $F(d_1, (0, 0)) = 0$. Through direct computation, the Fréchet derivative of F with respect to U at the trivial solution is given by

$$L(d_1) = F_U(d_1, (0, 0)) = \begin{pmatrix} d_1\Delta - 1 & 1 \\ -\dfrac{p\beta}{1 + c\beta} & d_2\Delta + h - \dfrac{2h\beta}{v_m} - \dfrac{p(1 + \beta)}{(1 + c\beta)^2} \end{pmatrix}, \quad \Delta = \frac{\mathrm{d}^2}{\mathrm{d}x^2},$$

whose characteristic equation corresponds to (2.4) in Section 2.

Throughout this subsection, we assume that

$$d_2\lambda_1 < h - \frac{2h\beta}{v_m} - \frac{p(1 + \beta)}{(1 + c\beta)^2}.$$

Under this condition, there exists the largest positive integer i_0, such that

$$d_2\lambda_i < h - \frac{2h\beta}{v_m} - \frac{p(1 + \beta)}{(1 + c\beta)^2}.$$

When $\mu = 0$ in (2.4) and $\Omega = (0, \pi)$, we have

$$(H) : d_1 = d_{1,i} = \frac{d_2\lambda_i + \left(-h + \dfrac{2h\beta}{v_m} + \dfrac{pc\beta^2 + 2p\beta + p}{(1 + c\beta)^2}\right)}{\lambda_i\left(h - \dfrac{2h\beta}{v_m} - \dfrac{p(1 + \beta)}{(1 + c\beta)^2} - d_2\lambda_i\right)}, \quad \lambda_i = i^2, \quad 1 \le i \le i_0.$$

We aim to establish the existence of non-constant positive solutions of $F(d_1, (s, v)) = 0$ in a neighborhood of $(d_{1,i}, (0, 0))$ for $1 \le i \le i_0$. Note that $d_{1,i}$ and $d_{1,j}$ may coincide or differ when $i \ne j$. The proof is carried out separately for bifurcations associated with simple and double eigenvalues.

Theorem 4.1. *Suppose that* (H) *is satisfied.*

(i) *For random integers* $i, j \in [1, i_0]$, *if* $i \ne j$ *implies* $d_{1,i} \ne d_{1,j}$, *then* $(d_{1,i}, (0, 0))$ *is a bifurcation point of* $F(d_1, U) = 0$. *When* $|b|$ *is sufficiently small, there is a curve of non-constant solutions* $(d_1(b), (s(b), v(b)))$ *of* $F(d_1, U) = 0$, *which satisfies* $d_1(0) = d_{1,i}$, $(s(0), v(0)) = (0, 0)$, $s(b) = b\phi_i + o(b)$, $v(b) = be_i\phi_i + o(b)$, *where* $d_1(b)$, $s(b)$, $v(b)$ *are continuously differentiable functions of* b, $\phi_i = \sqrt{\frac{2}{\pi}}\cos ix$, *and*

$$e_i = \frac{p\beta}{(1 + c\beta)\left(-d_2\lambda_i + h - \frac{2h\beta}{v_m} - \frac{p(1+\beta)}{(1+c\beta)^2}\right)}.$$

(ii) *Assume there exists a positive integer* $i \ne j$ *such that* $d_{1,i} = d_{1,j} = \hat{d}_1$. *Let*

$$e_i = \frac{p\beta}{(1 + c\beta)\left(-d_2\lambda_i + h - \dfrac{2h\beta}{v_m} - \dfrac{p(1 + \beta)}{(1 + c\beta)^2}\right)}, \tag{4.3}$$

$$e_i^* = \frac{1}{\lambda_i d_2 - h + \dfrac{2h\beta}{v_m} + \dfrac{p(1+\beta)}{(1+c\beta)^2}}, \quad \Phi_i = \begin{pmatrix} 1 \\ e_i \end{pmatrix} \phi_i, \tag{4.4}$$

$$A_1 = -\frac{p}{(1+cv)^2} e_i + \left(\frac{cps}{(1+cv)^3} - \frac{h}{v_m} \right) e_i^2, \tag{4.5}$$

$$A_2 = -\frac{p}{(1+cv)^2} (e_i + e_j) + 2\left(\frac{cps}{(1+cv)^3} - \frac{h}{v_m} \right) e_i e_j, \tag{4.6}$$

$$A_3 = -\frac{p}{(1+cv)^2} e_j + \left(\frac{cps}{(1+cv)^3} - \frac{h}{v_m} \right) e_j^2, \tag{4.7}$$

$$X_2 := \{(x,y)^T \in X : \int_0^\pi (x + e_i y)\phi_i \, \mathrm{d}x = \int_0^\pi (x + e_j y)\phi_j \, \mathrm{d}x = 0\}. \tag{4.8}$$

When $1 + e_i e_i^* \neq 0$, $1 + e_j e_j^* \neq 0$, *and* $j = 2i$ *(resp.* $i = 2j$*) hold, the point* $(\hat{d}_1, (0,0))$ *is a bifurcation point of* $F(d_1, U) = 0$. *In this case, a branch of non-constant solutions exists of the form*

$$(d_1(\omega),\ s(\omega)(\cos\omega\Phi_i + \sin\omega\Phi_j + W(\omega))),$$

for $|\omega - \omega_0|$ *sufficiently small, where the functions satisfy*

$$d_1(\omega_0) = \hat{d}_1, \quad s(\omega_0) = 0, \quad W(\omega_0) = 0,$$

and ω_0 *is any constant such that*

$$\tan^2\omega_0 \neq \frac{A_1(1 - e_j^*)i^2}{A_2(1 - e_i^*)j^2} \quad (\textit{resp.} \quad \tan^2\omega_0 \neq \frac{A_2(1 - e_j^*)i^2}{A_3(1 - e_i^*)j^2}), \tag{4.9}$$

where $d_1(\omega)$, $s(\omega)$, *and* $W(\omega)$ *are continuously differentiable with respect to* ω.

Proof. For the case of simple eigenvalues, we apply the Crandall-Rabinowitz bifurcation theorem as presented in [31]. It is straightforward to verify that the linear operators F_{d_1}, F_U, and $F_{d_1 U}$ exist and are continuous. Thus, we should notice that the operator

$$L(d_{1,i}) = F_U(d_{1,i}, (0,0)) = \begin{pmatrix} d_{1,i}\Delta - 1 & 1 \\ -\dfrac{p\beta}{1+c\beta} & d_2\Delta + h - \dfrac{2h\beta}{v_m} - \dfrac{p(1+\beta)}{(1+c\beta)^2} \end{pmatrix}, \quad \Delta = \frac{\mathrm{d}^2}{\mathrm{d}x^2}.$$

Assume arbitrary $\Phi_i = (\phi_i, e_i\phi_i) \in \ker L(d_{1,i})$, and we have

$$\ker L(d_{1,i}) = \mathrm{span}(\Phi_i), \quad \Phi_i = \begin{pmatrix} 1 \\ e_i \end{pmatrix} \phi_i,$$

where $e_i = \dfrac{p\beta}{(1+c\beta)(-d_2\lambda_i + h - \dfrac{2h\beta}{v_m} - \dfrac{p(1+\beta)}{(1+c\beta)^2})}$. Thus, $\dim\ker L(d_{1,i}) = 1$.

The adjoint operator of $L(d_{1,i})$ is defined by

$$L^*(d_{1,i}) = \begin{pmatrix} d_{1,i}\Delta - 1 & -\dfrac{p\beta}{1+c\beta} \\ 1 & d_2\Delta + h - \dfrac{2h\beta}{v_m} - \dfrac{p(1+\beta)}{(1+c\beta)^2} \end{pmatrix}, \quad \Delta = \frac{\mathrm{d}^2}{\mathrm{d}x^2}.$$

Similarly, for arbitrary $\Phi_i^* \in \ker L(d_{1,i})$, we have

$$\ker L^*(d_{1,i}) = \mathrm{span}\{\Phi_i^*\}, \quad \Phi_i^* = \begin{pmatrix} 1 \\ e_i^* \end{pmatrix} \phi_i,$$

where $e_i^* = \dfrac{1}{\lambda_i d_2 - h + \dfrac{2h\beta}{v_m} + \dfrac{p(1+\beta)}{(1+c\beta)^2}} < 0$. As we know, $R(L(d_{1,i})) = (\ker L^*(d_{1,i}))^{\perp}$. Thus,

$$\ker L^*(d_{1,i}) = \mathrm{span}\{\Phi_i^*\}, \quad \Phi_i^* = \begin{pmatrix} 1 \\ e_i^* \end{pmatrix} \phi_i.$$

Since

$$F_{d_1 U}(d_{1,i}, (0,0))\Phi_i = \begin{pmatrix} \Delta & 0 \\ 0 & 0 \end{pmatrix} \Phi_i = \begin{pmatrix} -\lambda_i \phi_i \\ 0 \end{pmatrix}$$

and

$$\langle F_{d_1 U}(d_{1,i}, (0,0))\Phi_i, \Phi_i^* \rangle = -\lambda_i \int_0^{\pi} \phi_i^2 \, \mathrm{d}x = -\lambda_i \neq 0, \tag{4.10}$$

$F_{d_1 U}(d_{1,i}, (0,0))\Phi_i \notin \mathcal{R}(L(d_{1,i}))$. Hence the proof of (i) is complete.

Rewrite the map $F : R^+ \times X \to Y$ by

$$F(d_1, U) = \begin{pmatrix} d_1 s'' + 1 + (v + v_*) - (s + s_*) \\ d_2 v'' + h(v + v_*)\left(1 - \dfrac{v + v_*}{v_m}\right) - p(s + s_*)\dfrac{v + v_*}{1 + c(v + v_*)} \end{pmatrix} = L(d_1) \begin{pmatrix} s \\ v \end{pmatrix} + \begin{pmatrix} F_1(s, v) \\ F_2(s, v) \end{pmatrix},$$

where $F_1(s, v) = 0$ and

$$F_2(s, v) = -\frac{p}{(1+cv)^2} sv + \left(\frac{pcs}{(1+cv)^3} - \frac{h}{v_m}\right) v^2 + \frac{pc}{(1+cv)^3} sv^2 - \frac{c^2 ps}{(1+cv)^4} v^3 + O(|v|^4, |v|^3|s|).$$

Suppose there exist distinct positive integers $i, j \in [1, i_0]$, such that $d_{1,i} = d_{1,j} = \tilde{d}_1$. Then, it follows that

$$\ker L(\tilde{d}) = \mathrm{span}\{\Phi_i, \Phi_j\}, \quad \ker L^*(\tilde{d}) = \mathrm{span}\{\Phi_i^*, \Phi_j^*\},$$

$$R(L(\tilde{d}_1)) = \{(s, v)^T \in Y : \int_0^{\pi} (s + e_i^* v)\phi_i \, \mathrm{d}x = \int_0^{\pi} (s + e_j^* v)\phi_j \, \mathrm{d}x = 0\}.$$

Thus, $\dim \ker L(\tilde{d}_1) = \mathrm{codim}\, R(L(\tilde{d}_1)) = 2$. Hence, the Crandall-Rabinowitz bifurcation theorem is not applicable. We proceed by applying space decomposition and the implicit function theorem to complete the proof.

Let $X_1 = \ker L(\tilde{d}_1)$, where $X_1 = \text{span}\{\Phi_i, \Phi_j\}$. X_2 is defined in (4.8). Next, we define an operator P on Y by

$$P\begin{pmatrix} s \\ v \end{pmatrix} = \frac{1}{1+e_ie_i^*}\left[\int_0^\pi (s+e_i^*v)\phi_i\,\mathrm{d}x\right]\Phi_i + \frac{1}{1+e_je_j^*}\left[\int_0^\pi (s+e_j^*v)\phi_j\,\mathrm{d}x\right]\Phi_j. \tag{4.11}$$

We have $R(P) = \text{span}\{\Phi_i, \Phi_j\} = X_1 \subset Y$ with $P^2 = P$. Hence, P defines a projection from Y onto X_1. Decompose Y as $Y = Y_1 \oplus Y_2$, where $Y_1 = R(P) = X_1$ and $Y_2 = \ker P = R(L(\tilde{d}))$. We seek solutions of $F(d_1, U) = 0$ in the following form

$$(s, v)^T = \alpha(\cos\omega\Phi_i + \sin\omega\Phi_j + W), \quad W = (w_1, w_2)^T \in X_2, \tag{4.12}$$

where $\alpha, \omega \in \mathbb{R}$ are parameters.

Then, the implicit function theorem is employed to establish the existence of non-constant pairs (s, v). Fix $\omega_0 \in \mathbb{R}$ temporarily, and define a nonlinear mapping $\mathcal{K}(d_1, \alpha, W; \tilde{\omega}) : \mathbb{R}\times\mathbb{R}\times X_2\times(\tilde{\omega}_0 - \delta, \tilde{\omega}_0 + \delta) \to Y$ by

$$\mathcal{K}(d_1, \alpha, W; \tilde{\omega}) = \alpha^{-1}F(d_1, \alpha(\cos\omega\Phi_i + \sin\omega\Phi_j + W)) = L(d_1)\begin{pmatrix} \cos\omega\Phi_i + \sin\omega\Phi_j + W \end{pmatrix} + \alpha\begin{pmatrix} 0 \\ \tilde{F}_2 \end{pmatrix},$$

where

$$\begin{aligned}\tilde{F}_2 =& -\frac{p}{(1+cv)^2}(\cos\omega\phi_i + \sin\omega\phi_j + w_1)\left(e_i\cos\omega\phi_i + e_j\sin\omega\phi_j + w_2\right)\\ &+\left(\frac{cps}{(1+cv)^3} - \frac{h}{v_m}\right)\left(e_i\cos\omega\phi_i + e_j\sin\omega\phi_j + w_2\right)^2 + O(\alpha).\end{aligned}$$

By some calculations, we have

$$\begin{aligned}&\mathcal{K}_{(d_1,\alpha,W)}(\tilde{d}_1, 0, 0; \omega_0)(d_1, \alpha, W) = L(\tilde{d}_1)W - d_1\lambda_i\cos\omega_0\begin{pmatrix}\phi_i\\0\end{pmatrix} - d_1\lambda_j\sin\omega_0\begin{pmatrix}\phi_j\\0\end{pmatrix}\\ &+\alpha A_1\cos^2\omega_0\begin{pmatrix}0\\\phi_i^2\end{pmatrix} + \alpha A_2\cos\omega_0\sin\omega_0\begin{pmatrix}0\\\phi_i\phi_j\end{pmatrix} + \alpha A_3\sin^2\omega_0\begin{pmatrix}0\\\phi_j^2\end{pmatrix},\end{aligned}$$

where A_1, A_2, and A_3 are given in (4.5)–(4.7).

We prove that $\mathcal{K}_{(d_1,\alpha,W)}(\tilde{d}_1, 0, 0; \tilde{\omega}_0) : \mathbb{R}\times\mathbb{R}\times X_2 \to Y$ is an isomorphism. We can rewrite

$$\mathcal{K}_{(d_1,\alpha,W)}(\tilde{d}_1, 0, 0; \omega_0)(d_1, \alpha, W) = \mathscr{Y}_1 + \mathscr{Y}_2, \quad \mathscr{Y}_1 \in Y_1 \quad \text{and} \quad \mathscr{Y}_2 \in Y_2,$$

and decompose

$$\begin{pmatrix}\phi_i\\0\end{pmatrix} = b_1\Phi_i + \begin{pmatrix}s_1\\v_1\end{pmatrix}, \quad \begin{pmatrix}\phi_j\\0\end{pmatrix} = b_2\Phi_j + \begin{pmatrix}s_2\\v_2\end{pmatrix},$$

where

$$\begin{pmatrix}s_1\\v_1\end{pmatrix} = \begin{pmatrix}1-b_1\\-b_1e_i\end{pmatrix}\phi_i, \quad b_1 = \frac{1}{1+e_ie_i^*} \neq 0,$$

$$\begin{pmatrix}s_2\\v_2\end{pmatrix} = \begin{pmatrix}1-b_2\\-b_2e_j\end{pmatrix}\phi_j, \quad b_2 = \frac{1}{1+e_je_j^*} \neq 0.$$

Next, we consider the case $j = 2i$. In this case, we get

$$\int_0^\pi \phi_i^2\phi_j \,\mathrm{d}x = \sqrt{\frac{1}{2\pi}}, \quad \int_0^\pi \phi_i\phi_j^2 \,\mathrm{d}x = 0 \quad \text{and} \quad \int_0^\pi \phi_i^3 \,\mathrm{d}x = \int_0^\pi \phi_j^3 \,\mathrm{d}x = 0,$$

$$\int_0^\pi \phi_i^2 \,\mathrm{d}x = \int_0^\pi \phi_j^2 \,\mathrm{d}x = 1, \quad \int_0^\pi \phi_i\phi_j \,\mathrm{d}x = 0.$$

Then, from (4.11), we can obtain $\begin{pmatrix} 0 \\ \phi_j^2 \end{pmatrix} \in Y_2$.

We further need to decompose

$$\begin{pmatrix} 0 \\ \phi_i^2 \end{pmatrix} = b_3\Phi_j + \begin{pmatrix} s_3 \\ v_3 \end{pmatrix}, \quad \begin{pmatrix} 0 \\ \phi_i\phi_j \end{pmatrix} = b_4\Phi_i + \begin{pmatrix} s_4 \\ v_4 \end{pmatrix},$$

where

$$b_3 = \frac{e_j^*}{e_j e_j^* + 1}\int_0^\pi \phi_i^2\phi_j \,\mathrm{d}x = \sqrt{\frac{1}{2\pi}}\frac{e_j^*}{e_j e_j^* + 1} \neq 0, \quad \begin{pmatrix} s_3 \\ v_3 \end{pmatrix} = \begin{pmatrix} -b_3\phi_j \\ \phi_i^2 - b_3 e_j\phi_j \end{pmatrix} \in Y_2,$$

$$b_4 = \frac{e_i^*}{e_i e_i^* + 1}\int_0^\pi \phi_i^2\phi_j \,\mathrm{d}x = \sqrt{\frac{1}{2\pi}}\frac{e_i^*}{e_i e_i^* + 1} \neq 0, \quad \begin{pmatrix} s_4 \\ v_4 \end{pmatrix} = \begin{pmatrix} -b_4\phi_i \\ \phi_i\phi_j - b_4 e_i\phi_i \end{pmatrix} \in Y_2.$$

Then, we get

$$\mathscr{Y}_1 = (-d_1 b_1\lambda_i \cos\omega_0 + \alpha b_4 A_2 \cos\omega_0 \sin\omega_0)\Phi_i + (-d_1 b_2\lambda_j \sin\omega_0 + \alpha b_3 A_1 \cos^2\omega_0)\Phi_j \in Y_1,$$

$$\begin{aligned}\mathscr{Y}_2 =& L(\tilde{d}_1)W - d_1\lambda_i \cos\omega_0 \begin{pmatrix} s_1 \\ v_1 \end{pmatrix} - d_1\lambda_j \sin\omega_0 \begin{pmatrix} s_2 \\ v_2 \end{pmatrix} + \alpha A_1 \cos^2\omega_0 \begin{pmatrix} s_3 \\ v_3 \end{pmatrix} \\ &+ \alpha A_2 \cos\omega_0 \sin\omega_0 \begin{pmatrix} s_4 \\ v_4 \end{pmatrix} + \alpha A_3 \sin^2\omega_0 \begin{pmatrix} 0 \\ \phi_j^2 \end{pmatrix} \in Y_2.\end{aligned}$$

Let

$$\mathcal{K}_{(d_1,\alpha,W)}(\tilde{d}_1, 0, 0; \omega_0)(d_1, \alpha, W) = 0. \tag{4.13}$$

Then, (4.13) is equivalent to $\mathscr{Y}_1 = 0$ and

$$\begin{cases} (-d_1 b_1\lambda_i \cos\omega_0 + \alpha b_4 A_2 \cos\omega_0 \sin\omega_0)\Phi_i + (-d_1 b_2\lambda_j \sin\omega_0 + \alpha b_3 A_1 \cos^2\omega_0)\Phi_j = 0, \\ L(\tilde{d}_1)W - d_1\lambda_i \cos\omega_0 \begin{pmatrix} s_1 \\ v_1 \end{pmatrix} - d_1\lambda_j \sin\omega_0 \begin{pmatrix} s_2 \\ v_2 \end{pmatrix} + \alpha A_1 \cos^2\omega_0 \begin{pmatrix} s_3 \\ v_3 \end{pmatrix} \\ +\alpha A_2 \cos\omega_0 \sin\omega_0 \begin{pmatrix} s_4 \\ v_4 \end{pmatrix} + \alpha A_3 \sin^2\omega_0 \begin{pmatrix} 0 \\ \phi_j^2 \end{pmatrix} = 0. \end{cases} \tag{4.14}$$

Moreover, $d_1 = 0$, $s = 0$ follows from $\mathscr{Y}_1 = 0$. Substituting into $\mathscr{Y}_2 = 0$ yields $W = 0$. Thus, $\mathcal{K}_{(d_1,\alpha,W)}(\tilde{d}_1, 0, 0; \tilde{\omega}_0)$ is injective. We now show that $\mathcal{K}_{(d_1,\alpha,W)}(\tilde{d}_1, 0, 0; \tilde{\omega}_0)$ is surjective.

Given a random vector $\begin{pmatrix} s \\ v \end{pmatrix} \in Y$, we determine $(d_1, \alpha, W) \in \mathbb{R} \times \mathbb{R} \times X_2$, such that

$$\mathcal{K}_{(d_1,\alpha,W)}(\tilde{d}_1, 0, 0; \tilde{\omega}_0)(d_1, \alpha, W) = \begin{pmatrix} s \\ v \end{pmatrix}. \tag{4.15}$$

Based on the decomposition of Y, there exist $\eta, \gamma \in \mathbb{R}$ and $(s_0, v_0) \in Y_2$, such that

$$\begin{pmatrix} s \\ v \end{pmatrix} = \begin{pmatrix} s_0 \\ v_0 \end{pmatrix} + \eta\Phi_i + \gamma\Phi_j.$$

Substituting it into (4.14) gets

$$\begin{cases} -d_1 b_1 \lambda_i \cos\omega_0 + \alpha b_4 A_2 \cos\omega_0 \sin\omega_0 = \eta, \\ -d_1 b_2 \lambda_j \sin\omega_0 + \alpha b_3 A_1 \cos^2\omega_0 = \gamma, \\ L(\tilde{d}_1)W - d_1\lambda_i \cos\omega_0 \begin{pmatrix} s_1 \\ v_1 \end{pmatrix} - d_1\lambda_j \sin\omega_0 \begin{pmatrix} s_2 \\ v_2 \end{pmatrix} + \alpha A_1 \cos^2\omega_0 \begin{pmatrix} s_3 \\ v_3 \end{pmatrix} \\ +\alpha A_2 \cos\omega_0 \sin\tilde{\omega}_0 \begin{pmatrix} s_4 \\ v_4 \end{pmatrix} + \alpha A_3 \sin^2\omega_0 \begin{pmatrix} 0 \\ \phi_j^2 \end{pmatrix} = \begin{pmatrix} s_0 \\ v_0 \end{pmatrix}. \end{cases} \tag{4.16}$$

Because ω_0 satisfies (4.9) and (4.16) holds, when $j = 2i$, we obtain

$$d_1 = \bar{d}_1 := \frac{\eta b_3 A_1 \cos\omega_0 - \gamma b_4 \sin\omega_0}{b_2 b_4 \lambda_j A_2 \sin^2\omega_0 - b_1 b_3 \lambda_i A_1 \cos^2\omega_0},$$

$$\alpha = \bar{\alpha} := \frac{\eta b_2 \lambda_j \sin\tilde{\omega}_0 - \gamma c_1 \lambda_i \cos\tilde{\omega}_0}{c_2 b_4 \lambda_j A_2 \sin^2\tilde{\omega}_0 \cos\tilde{\omega}_0 - b_1 b_3 \lambda_i A_1 \cos^3\tilde{\omega}_0}.$$

Substituting $\bar{d}_1$ and $\bar{\alpha}$ into the third equation of (4.16), we get

$$L(\widetilde{d_1})W = \begin{pmatrix} s_0 \\ v_0 \end{pmatrix} + \bar{d}_1\lambda_i \cos\omega_0 \begin{pmatrix} s_1 \\ v_1 \end{pmatrix} + \bar{d}_1\lambda_j \sin\omega_0 \begin{pmatrix} s_2 \\ v_2 \end{pmatrix} - \bar{\alpha} A_1 \cos^2\omega_0 \begin{pmatrix} s_3 \\ v_3 \end{pmatrix} -$$

$$\bar{\alpha} A_2 \cos\omega_0 \sin\omega_0 \begin{pmatrix} s_4 \\ v_4 \end{pmatrix} - \bar{\alpha} A_3 \sin^2\omega_0 \begin{pmatrix} 0 \\ \phi_j^2 \end{pmatrix} := \begin{pmatrix} \bar{s} \\ \bar{v} \end{pmatrix} \in Y_2.$$

Then,

$$(d_1, \alpha, W) = (\bar{d}_1, \bar{\alpha}, L^{-1}\begin{pmatrix} \bar{s} \\ \bar{v} \end{pmatrix}),$$

satisfies (4.15). This confirms that $\mathcal{K}_{(d_1,\alpha,W)}(\tilde{d}_1, 0, 0; \tilde{\omega}_0)$ is surjective.

Consequently, $\mathcal{K}_{(d_1,\alpha,W)}(\tilde{d}_1, 0, 0; \omega_0)$ is an isomorphism. We apply the implicit theorem for

$$\mathcal{K}(d_1, \alpha, W; \omega) = 0. \tag{4.17}$$

There is a curve of non-constant solutions $(d_1(\omega), \alpha(\omega), W(\omega))$ of (4.16) (i.e., $\tilde{F} = 0$) in a small neighborhood of $\tilde{\omega}_0$, where ω_0 satisfies $d_1(\omega_0) = \tilde{d}_1$, $\alpha(\omega_0) = 0$, $W(\omega_0) = 0$. $d_1(\omega), \alpha(\omega), W(\omega)$ are continuously differentiable functions with respect to ω and $W \in X_2$.

Due to the invariance of the problem under the transformation $(i, j, \omega) \mapsto (j, i, \frac{\pi}{2} - \omega)$, it suffices to consider only the case $j = 2i$. The case $i = 2j$ follows by symmetry and is omitted for brevity.

Remark 4.1. *It is a pity that we cannot show the existence of non-constant positive solutions to (4.1) when $i \neq 2j$ and $j \neq 2i$. In this case, we can get $\int_0^\pi \phi_i^2\phi_j \mathrm{d}x = \int_0^\pi \phi_j^2\phi_i \mathrm{d}x = 0$, which implies*

$$\begin{pmatrix} -\phi_i^2 \\ \phi_i^2 \end{pmatrix}, \begin{pmatrix} -\phi_j^2 \\ \phi_j^2 \end{pmatrix} \quad \text{and} \quad \begin{pmatrix} -\phi_i\phi_j \\ \phi_i\phi_j \end{pmatrix} \in Y_2.$$

At this stage, $\mathcal{K}_{(d_1,\alpha,W)}(\tilde{d}_1, 0, 0; \omega_0) : \mathbb{R}^+ \times \mathbb{R} \times X_2 \to Y$ is not an isomorphism. As a result, the implicit function theorem is inapplicable to establish the existence when $i \neq 2j$ and $j \neq 2i$.

4.2. The global structure of non-constant positive solutions

In this subsection, we extend the local bifurcation result to a global one associated with simple eigenvalues. To explore the global structure, let J be the closure of the non-constant solution set of (4.1) and define Υ_i as the connected component of $J \cup \{(d_{1,i}, (s_*, v_*))\}$.

Theorem 4.2. *Assume the conditions of Theorem 4.1 (i) hold. Then, the projection of Υ_i onto the d_1-axis contains the interval $(d_{1,i}, +\infty)$. In particular, for any integer $j \geq 1$ and $d_1 > \tilde{d}_1$ with $d_1 \neq d_{1,j}$, where $\tilde{d}_1$ is defined in (2.3), system (4.1) admits at least one non-constant positive solution.*

Proof. Rewrite (4.2) as

$$\begin{cases} -d_1 s'' = v - s, \quad x \in (0, \pi), \\ -d_2 v'' = -\dfrac{p\beta}{1 + c\beta} s + \left(h - \dfrac{2h\beta}{v_m} - \dfrac{p(1+\beta)}{(1+c\beta)^2} \right) v + f_2(s, v), \quad x \in (0, \pi). \end{cases} \tag{4.18}$$

First, define the following two mappings

$$\begin{cases} J_{d_1} : \rho \to \theta, \quad \theta - d_1\theta'' = \rho, \\ \\ J_{d_2} : \rho \to \theta, \quad (h - \dfrac{2h\beta}{v_m} - \dfrac{p(1+\beta)}{(1+c\beta)^2})\theta - d_2\theta'' = \rho. \end{cases}$$

After this mapping, (4.18) can be transformed into the following equation

$$U = K(d_1)U + M(U), \tag{4.19}$$

where

$$K(d_1)U = \left(J_{d_1}(v), -\frac{p\beta}{1 + c\beta} J_{d_2}(s) + 2H\, J_{d_2}(v) \right)^T, \quad M(U) = \left(0, J_{d_2}(f_2(s, v))\right)^T,$$

with $H = h - \dfrac{2h\beta}{v_m} - \dfrac{p(1+\beta)}{(1+c\beta)^2}$. Both $K(d_1)$ and M are compact on X, and $M(U) = o(|U|)$ near 0 uniformly in d_1.

By the Rabinowitz's global bifurcation theorem (Theorem 1.3 in [32]) and Theorem 4.1 (i), we know that $\ker(K(d_{1,i}) - I) = \mathrm{span}\{\Phi_i\}$ and $\dim \ker(K(d_{1,i}) - I) = 1$. We aim to show that

$$\ker(K(d_{1,i}) - I) \cap R(K(d_{1,i}) - I) = 0. \tag{4.20}$$

Thus, (4.20) is satisfied.

Let $\ker(K^*(d_{1,i}))$ be the adjoint operator of $K(d_{1,i})$. For any $(\gamma, \zeta) \in \ker(K^*(d_{1,i}) - I)$, then we have

$$-\frac{p\beta}{1+c\beta} J_{d_2}(\zeta) = \gamma, \quad J_{d_1}(\gamma) + 2H\, J_{d_2}(\zeta) = \zeta.$$

This implies

$$-d_2\gamma'' = -H\gamma - \frac{p\beta}{1+c\beta}\zeta, \quad -d_{1,i}\zeta'' = A\gamma - B\zeta,$$

where A and B are constants depending on the parameters.

Expanding $\gamma = \sum a_j\phi_j$ and $\zeta = \sum b_j\phi_j$, we get

$$\sum_{j\geq 0} B_j^* \begin{pmatrix} a_j \\ b_j \end{pmatrix} \phi_j = 0, \tag{4.21}$$

with

$$B_j^* = \begin{pmatrix} -H - d_2\lambda_j & -N \\ 1 - \frac{2H}{N}\left(1 + \frac{d_{1,i}H}{d_2}\right) & -\frac{1+c\beta+p\beta}{1+c\beta} d_2 - d_{1,i}\lambda_j \end{pmatrix}, \quad N = \frac{p\beta}{1+c\beta}.$$

Thus, $\ker(K^*(d_{1,i}) - I) = \operatorname{span}\{\Phi_i'\}$, where

$$\Phi_i' = \left(-\frac{p\beta}{1+c\beta}, H + d_2\lambda_j\right)^T \phi_i.$$

Since

$$\int_0^\pi \Phi_i^T \Phi_i'\, dx = \frac{p\beta}{1+c\beta}\left(-1 + \frac{H + d_2\lambda_j}{H - d_2\lambda_j}\right) < 0,$$

we conclude that $\Phi_i \notin R(K(d_{1,i}) - I)$, hence (4.20) holds.

When d_1 is close to $d_{1,i}$, the operator $I - K(d_1)$ is bijective, and 0 is an isolated solution of (4.19). Define

$$i(I - K(d_1) - J, (d_1, 0)) = \deg(I - K(d_1), B, 0) = (-1)^q,$$

where q is the total algebraic multiplicity of eigenvalues of $K(d_1)$ greater than 1.

To see that the index changes across $d_{1,i}$, suppose μ is an eigenvalue of $K(d_1)$, then

$$-\mu d_1\gamma'' = -\mu\gamma + \zeta, \quad -\mu d_2\zeta'' = -\frac{p\beta}{1+c\beta}\gamma + (2-\mu)H\zeta.$$

As in (4.21), this yields a characteristic equation

$$(H + d_2\lambda_j)\mu^2 - 2H\mu + \frac{p\beta}{(1+d_1\lambda_j)(1+c\beta)} = 0. \tag{4.22}$$

For $d_1 = d_{1,i}$, one root of (4.22) is $\mu = 1$ iff $j = i$. For d_1 near $d_{1,i}$, the number and multiplicity of $\mu > 1$ eigenvalues of $K(d_1)$ remain unchanged except at $j = i$, where the eigenvalue crosses 1 as d_1 varies. Thus,

$$i(I - K(d_{1,i} + \varepsilon) - J, (d_{1,i} + \varepsilon, 0)) \neq i(I - K(d_{1,i} - \varepsilon) - J, (d_{1,i} - \varepsilon, 0)).$$

Therefore, by Theorem 1.3 in [32], Υ_i either meets another bifurcation point $(d_k, (s_*, v_*))$ with $k \neq i$, or is unbounded in $\mathbb{R} \times X$.

To exclude the first case, assume Υ_i is bounded and intersects only finitely many bifurcation points. Choose $j > z$ such that Υ_i meets $(d_z, (s_*, v_*))$ but not $(d_j, (s_*, v_*))$. Consider (4.1) on $(0, \pi/z)$, then we have

$$\begin{cases} -d_1 s'' = 1 + v - s, & x \in (0, \pi/z), \\ -d_2 v'' = hv\left(1 - \dfrac{v}{v_m}\right) - ps\dfrac{v}{1 + cv}, & x \in (0, \pi/z), \\ s' = v' = 0, & x \in (0, \pi/z). \end{cases} \tag{4.23}$$

Let $\widetilde{N}$ be a solution of (4.23). Using periodic-reflective extension as in [33, 34], we construct $\bar{N}$ on $(0, \pi)$. Let

$$\widetilde{d}_{1,i} = \frac{d_2\widetilde{\lambda}_i + \left(-h + \dfrac{2h\beta}{v_m} + \dfrac{pc\beta^2 + 2p\beta + p}{(1 + c\beta)^2}\right)}{\widetilde{\lambda}_i(H - d_2\widetilde{\lambda}_i)},$$

where $\widetilde{\lambda}_i = (iz)^2 = \lambda_{zi}$; hence, $\widetilde{d}_{1,i} = d_{1,zi}$. In particular, $\widetilde{d}_{1,1} = d_{1,z}$ is a bifurcation point of (4.23). Let χ_z be the bifurcation branch from $(\widetilde{d}_{1,1}, (s_*, v_*))$.

By the same reasoning, either χ_z meets infinity or intersects $(d_{1,\alpha z}, (s_*, v_*))$ for some $\alpha > 1$. The latter implies that Υ_i also meets this point, contradicting our assumption on $j > z$. Thus, χ_z is unbounded, and so is Υ_i. The proof is complete.

Remark 4.2. *Theorem 4.2 rules only out the possibility that Υ_i finally meets some bifurcation points without reaching infinity. Υ_i maybe meets some bifurcation points and then reaches infinity.*

4.3. Direction of the bifurcation

In this part, for the simple eigenvalues obtained in Theorem 4.1 (i), we mainly give the judgment condition of the direction of the steady-state bifurcations.

Define the map $F : \mathbb{R}^+ \times X \to Y$ by

$$F(d_1, U) = \begin{pmatrix} d_1 s'' + \tilde{f}(s, v) \\ d_2 v'' + \tilde{g}(s, v) \end{pmatrix},$$

where

$$\begin{cases} \tilde{f}(s, v) = 1 + (v + v_*) - (s + s_*), \\ \tilde{g}(s, v) = h(v + v_*)\left(1 - \dfrac{v + v_*}{v_m}\right) - p(s + s_*)\dfrac{v + v_*}{1 + c(v + v_*)}. \end{cases}$$

Through simple calculations, we have

$$\tilde{f}_s(0,0) = -1, \quad \tilde{f}_v(0,0) = 1, \quad \tilde{g}_s(0,0) = -\frac{p\beta}{1 + c\beta}, \quad \tilde{g}_v(0,0) = h - \frac{2h\beta}{v_m} - \frac{p(1+\beta)}{(1 + c\beta)^2},$$

$$\tilde{g}_{ss}(0,0) = 0, \quad \tilde{g}_{sv}(0,0) = -\frac{p}{(1 + c\beta)^2}, \quad \tilde{g}_{vv}(0,0) = -\frac{2h}{v_m} + \frac{2pc(1+\beta)}{(1 + c\beta)^3},$$

$$\tilde{g}_{sss}(0,0) = 0, \quad \tilde{g}_{ssv}(0,0) = 0, \quad \tilde{g}_{svv}(0,0) = \frac{2pc}{(1 + c\beta)^3}, \quad \tilde{g}_{vvv}(0,0) = -\frac{6c^2 p(1+\beta)}{(1 + c\beta)^4}.$$

Based on Theorem 4.1 (i), we know that

$$\dim\ker F_U(d_{1,i},(0,0)) = \mathrm{codim}R(F_U(d_{1,i},(0,0))) = 1,$$

and $\ker F_U(d_{1,i},(0,0)) = \mathrm{span}\{\Phi_i\}$. Hence, X and Y admit the following decomposition

$$X = \ker F_U(d_{1,i},(0,0)) \oplus Q \quad \text{and} \quad Y = R(F_U(d_{1,i},(0,0)) \oplus Q',$$

where Q is the supplement of $\ker F_U(d_{1,i},(0,0))$ in X, and Q' is the supplement of $R(F_Q(d_{2,i},(0,0))$ in Y. By the formula (4.7) in [35], we have

$$d_1'(0) = -\frac{\langle F_{UU}(d_{1,i},(0,0))\Phi_i^2, \Phi_i^*\rangle}{2\langle F_{d_1U}(d_{1,i},(0,0))\Phi_i, \Phi_i^*\rangle}.$$

By (4.10), we get

$$\langle F_{d_1U}(d_{1,i},(0,0))\Phi_i, \Phi_i^*\rangle = -\lambda_i = -i^2 \neq 0.$$

Then, by calculations, we get

$$\langle F_{UU}(d_{1,i},(0,0))\Phi_i^2, \Phi_i^*\rangle = (m_i + r_i e_i^*)\int_0^\pi \phi_i^3\, dx,$$

where $m_i = 0$ and

$$r_i = \tilde{g}_{ss}(0,0) + 2\tilde{g}_{sv}(0,0)e_i + \tilde{g}_{vv}(0,0)e_i^2 = -\frac{2p}{(1+c\beta)^2}e_i + \left(\frac{2cp(1+\beta)}{(1+c\beta)^3} - \frac{2h}{v_m}\right)e_i^2. \tag{4.24}$$

Since $\int_0^\pi \phi_i^3 \mathrm{d}x = 0$, we have $\langle F_{UU}(d_{1,i},(0,0))\Phi_i^2, \Phi_i^*\rangle = 0$. Then, $d_1^{'}(0) = 0$.

In such case, based on the formula (4.8) in [35], we need to see

$$d_1''(0) = -\frac{\langle F_{UUU}(d_{1,i},(0,0))\Phi_i^3, \Phi_i^*\rangle + 3\langle F_{UU}(d_{1,i},(0,0))\Phi_i\theta, \Phi_i^*\rangle}{3\langle F_{d_1U}(d_{1,i},(0,0))\Phi_i, \Phi_i^*\rangle},$$

where θ satisfies

$$F_{UU}(d_{1,i},(0,0))\Phi_i^2 + F_U(d_{1,i},(0,0))\theta = 0.$$

If $d_1''(0) < (>)0$, the direction of the steady-state bifurcation is supercritical (resp. subcritical). A direct calculation gives us

$$\langle F_{UUU}(d_{1,i},(0,0))\Phi_i^3, \Phi_i^*\rangle = \frac{4}{\pi^2}(n_i + k_i e_i^*)\int_0^\pi \cos^4(ix)\, dx = \frac{3}{2\pi}(n_i + k_i e_i^*),$$

where $n_i = 0$ and

$$\begin{aligned} k_i &= \tilde{g}_{sss}(0,0) + 3\tilde{g}_{ssv}(0,0)e_i + 3\tilde{g}_{svv}(0,0)e_i^2 + \tilde{g}_{vvv}(0,0)e_i^3 \\ &= \frac{6pc}{(1+c\beta)^3}e_i^2 - \frac{6c^2p(1+\beta)}{(1+c\beta)^4}e_i^3. \end{aligned} \tag{4.25}$$

Let $\theta = (\theta_1, \theta_2)$, then θ satisfies

$$\begin{cases} d_{1,i}\theta_1'' + \tilde{f}_s(0,0)\theta_1 + \tilde{f}_v(0,0)\theta_2 = -m_i\phi_i^2 = 0, & x \in (0,\pi), \\ d_2\theta_2'' + \tilde{g}_s(0,0)\theta_1 + \tilde{g}_v(0,0)\theta_2 = -r_i\phi_i^2, & x \in (0,\pi), \\ \theta_i'(0) = \theta_i'(\pi) = 0, \quad i = 1,2. \end{cases} \tag{4.26}$$

Integrating (4.26) on $[0,\pi]$, we have

$$\int_0^\pi \theta_1 \,\mathrm{d}x = \frac{r_i\tilde{f}_v(0,0) - m_i\tilde{g}_v(0,0)}{\tilde{f}_s(0,0)\tilde{g}_v(0,0) - \tilde{f}_v(0,0)\tilde{g}_s(0,0)} = \frac{r_i}{\mathrm{Det}J}, \tag{4.27}$$

$$\int_0^\pi \theta_2 \,\mathrm{d}x = \frac{m_i\tilde{g}_s(0,0) - r_i\tilde{f}_s(0,0)}{\tilde{f}_s(0,0)\tilde{g}_v(0,0) - \tilde{f}_s(0,0)\tilde{g}_v(0,0)} = \frac{r_i}{\mathrm{Det}J}. \tag{4.28}$$

From direct calculations, we have

$$\langle F_{UU}(d_{1,i},(0,0))\Phi_i\theta, \Phi_i^*\rangle = C_1\int_0^\pi \theta_1\phi_i^2\,dx + C_2\int_0^\pi \theta_2\phi_i^2\,dx,$$

where

$$C_1 = \tilde{f}_{ss}(0,0) + \tilde{f}_{sv}(0,0)e_i + (\tilde{g}_{ss}(0,0) + \tilde{g}_{vs}(0,0)e_i)e_i^*,$$
$$C_2 = \tilde{f}_{sv}(0,0) + \tilde{f}_{vv}(0,0)e_i + (\tilde{g}_{sv}(0,0) + \tilde{g}_{vv}(0,0)e_i)e_i^*.$$

By the definitions of e_i, e_i^*, we have

$$C_1 = \tilde{g}_{sv}(0,0)e_ie_i^* = \frac{p^2\beta}{(1+c\beta)^3(-d_2\lambda_i + h - \frac{2h\beta}{v_m} - \frac{p(1+\beta)}{(1+c\beta)^2})^2},$$

$$C_2 = (\tilde{g}_{sv}(0,0) + \tilde{g}_{vv}(0,0)e_i)e_i^*$$
$$= (d_2\lambda_i - h + \frac{2h\beta}{v_m} + \frac{p(1+\beta)}{(1+c\beta)^2})^{-1}\left(\frac{p\beta\left(\frac{2cp(1+\beta)}{(1+c\beta)^3} - \frac{2h}{v_m}\right)}{(1+c\beta)(-d_2\lambda_i + h - \frac{2h\beta}{v_m} - \frac{p(1+\beta)}{(1+c\beta)^2})} - \frac{p}{(1+c\beta)^2}\right).$$

Based on the above calculation process, we need to know the following integral result

$$\int_0^\pi \theta_1\phi_i^2\,dx \quad \text{and} \quad \int_0^\pi \theta_2\phi_i^2\,dx.$$

Multiplying (4.26) by ϕ_i^2 and noting that

$$\int_0^\pi \phi_i^4\,dx = \int_0^\pi \frac{4}{\pi^2}\cos^4(ix)\,dx = \frac{3}{2\pi},$$

then we have

$$d_{1,i}\int_0^\pi \theta_1''\phi_i^2\,\mathrm{d}x + \tilde{f}_s(0,0)\int_0^\pi \theta_1\phi_i^2\,\mathrm{d}x + \tilde{f}_v(0,0)\int_0^\pi \theta_2\phi_i^2\,\mathrm{d}x = 0, \tag{4.29}$$

and

$$d_2\int_0^\pi \theta_2''\phi_i^2\,\mathrm{d}x+\tilde{g}_s(0,0)\int_0^\pi \theta_1\phi_i^2\,\mathrm{d}x+\tilde{g}_v(0,0)\int_0^\pi \theta_2\phi_i^2\,\mathrm{d}x=-\frac{3}{2\pi}r_i. \tag{4.30}$$

Using integration by parts, we calculate that

$$\int_0^\pi \theta_j''\phi_i^2\,\mathrm{d}x=\frac{4i^2}{\pi}\int_0^\pi \theta_j(1-\pi\phi_i^2)\,\mathrm{d}x,\quad j=1,2. \tag{4.31}$$

Substituting (4.27), (4.28), and (4.31) into (4.29) and (4.30) and arranging terms yields

$$(\tilde{f}_s(0,0)-4i^2d_{1,i})\int_0^\pi \theta_1\phi_i^2\,dx+\tilde{f}_v(0,0)\int_0^\pi \theta_2\phi_i^2\,dx=-\frac{4i^2r_i}{\pi\mathrm{Det}J}d_{1,i},$$

and

$$\tilde{g}_s(0,0)\int_0^\pi \theta_1\phi_i^2\,dx+(\tilde{g}_v(0,0)-4i^2d_2)\int_0^\pi \theta_2\phi_i^2\,dx=-\frac{3}{2\pi}r_i-\frac{4i^2r_i}{\pi\mathrm{Det}J}d_2.$$

Solve the above binary linear equation system and then we get

$$\beta_1\triangleq\int_0^\pi \theta_1\phi_i^2\,dx=\frac{-8i^2r_id_{1,i}\tilde{g}_v(0,0)+32i^4r_id_{1,i}d_2+3r_i\mathrm{Det}J+8i^2r_id_2}{2\pi\mathrm{Det}J(\mathrm{Det}J-4i^2d_2\tilde{f}_s(0,0)-4i^2d_{1,i}\tilde{g}_v(0,0)+16i^4d_{1,i}d_2)},$$

$$\beta_2\triangleq\int_0^\pi \theta_2\phi_i^2\,dx=\frac{3\mathrm{Det}Jr_i+8i^2r_id_2+12\mathrm{Det}Ji^2r_id_{1,i}+32i^4r_id_{1,i}d_2+8i^2r_id_{1,i}\tilde{g}_s(0,0)}{2\pi\mathrm{Det}J(\mathrm{Det}J-4i^2d_2\tilde{f}_s(0,0)-4i^2d_{1,i}\tilde{g}_v(0,0)+16i^4d_{1,i}d_2)}.$$

By calculating the expression of $d_{1,i}$, we find

$$\mathrm{Det}J-4i^2d_2\tilde{f}_s(0,0)-4i^2d_{1,i}\tilde{g}_v(0,0)+16i^4d_{1,i}d_2$$

$$=\frac{p\beta}{1+c\beta}+4i^2d_2+16i^4d_{1,i}d_2-(1+4i^2d_{1,i})\left(h-\frac{2h\beta}{v_m}-\frac{p(1+\beta)}{(1+c\beta)^2}\right).$$

Thus, we have

$$d_1''(0)=\frac{6pc(1+c\beta)e_i^2e_i^*-6c^2p(1+\beta)e_i^3e_i^*+2\pi(1+c\beta)^4(C_1\beta_1+C_2\beta_2)}{2\pi\lambda_i(1+c\beta)^4}. \tag{4.32}$$

Note that the sign of $d_1''(0)$ determines the direction of the bifurcation.

Theorem 4.3. *Assume that $H<1$ and $H<N$. If $d_1''(0)>0$, the bifurcation from $(d_{1,i},(0,0))$ obtained in Theorem 4.1 (i) is supercritical. If $d_1''(0)<0$, it is subcritical.*

5. Numerical simulations

In this section, we present a series of numerical simulations designed to validate and illustrate the analytical results obtained in the previous sections. These simulations aim to provide visual confirmation of bifurcation phenomena, support theoretical predictions, and offer biological interpretations of the vegetation model's dynamics.

5.1. *Hopf bifurcation*

The parameters are chosen as $h = 24.65,\ p = 17,\ v_m = 10,\ c = 0.2$. When $H < 1$ and $H < N$, the equilibrium $(s_*, v_*) = (1.52, 0.52)$ of system (2.1) exhibits local asymptotic stability, as illustrated in Figure 1. For $h = 26$, with the same values of p, v_m, and c, the equilibrium (s_*, v_*) becomes unstable in system (2.1) (see Figure 2).

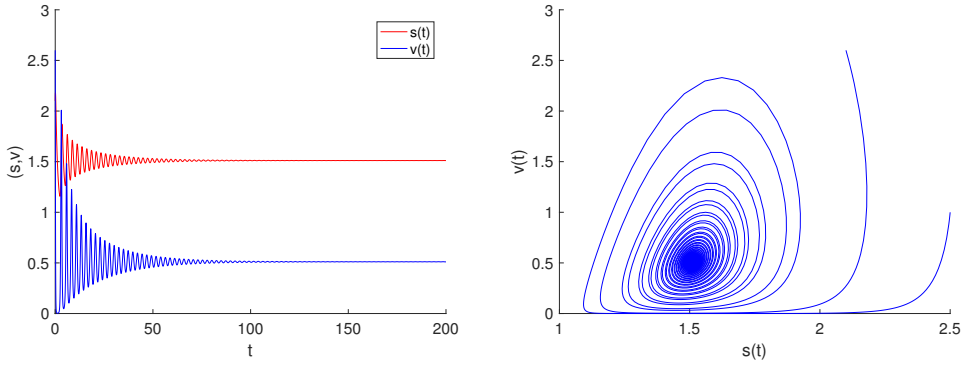

(a) Time evolution. **(b)** Phase diagram.

Figure 1. For $h = 24.56,\ p = 17,\ v_m = 10,\ c = 0.2$, the equilibrium (s_*, v_*) of system (2.1) exhibits local asymptotic stability.

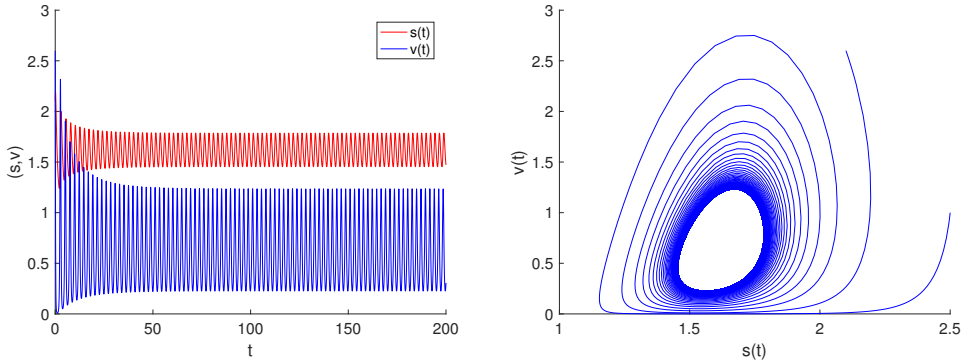

(a) Time evolution. **(b)** Phase diagram.

Figure 2. System (2.1) produces the stable periodic orbits under the parameter setting $h = 26,\ p = 17,\ v_m = 10,\ c = 0.2$.

5.2. *Steady-state bifurcation*

Rewriting $\Omega = (0, \pi)$, by Theorem 4.1, we obtain the neutral curves

$$d_{1,i} = \frac{d_2 i^2 + (-h + \dfrac{2h\beta}{v_m} + \dfrac{pc\beta^2 + 2p\beta + p}{(1+c\beta)^2})}{(h - \dfrac{2h\beta}{v_m} - \dfrac{p(1+\beta)}{(1+c\beta)^2} - d_2 i^2) i^2}, \quad 1 < i < i_0.$$

The neutral curves $d_{1,i}$ on $i \in [0.8, 2.3]$ are shown in Figure 3. It is observed from Figure 3(a) that $d_{1,1} \neq d_{1,2}$ and from Figure 3(b) that $d_{1,1} = d_{1,2}$. By letting $d_2 = 0.11$, we have $d_{1,1} = 6.556$ and $d_{1,2} = 1.967$.

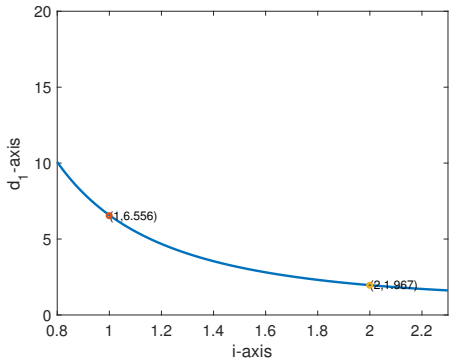

(a) Simple bifurcation case with $d_2 = 0.11$.

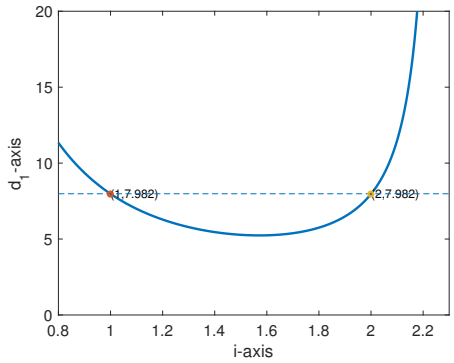

(b) Double bifurcation case with $d_2 = 0.04$.

Figure 3. Neutral curves $d_1(i)$ of system (1.4) for $h = 3.33$, $v_m = 10$, $p = 2.12$, $c = 1.11$.

According to Theorem 4.1(i), there are two simple bifurcation points $(d_{1,1}, (s_*, v_*))$ and $(d_{1,2}, (s_*, v_*))$ in Figure 3(a), and steady-state bifurcations occur at $d_1 = d_{1,i}, i = 1, 2$. By Theorem 4.3, the direction of bifurcation from $(d_{1,1}, (s_*, v_*))$ is subcritical, while the direction of bifurcation from $(d_{1,2}, (s_*, v_*))$ is supercritical. These results are shown in Figures 4 and 5. Assuming $h = 3.33$, $v_m = 10$, $p = 2.12$, and $c = 1.11$, the initial condition in Figure 4 is given by $(s_0, v_0) = (5.15 + 1.35\cos(1.7x), 4.15 + 1.35\cos(1.7x))$, showing spatial oscillations of the subcritical solution bifurcating from the simple eigenvalue $d_{1,1} = 6.56$. In Figure 5, the initial condition is $(s_0, v_0) = (5.15 + 2.64\cos(1.7x), 4.15 + 2.64\cos(1.7x))$, showing the supercritical branch bifurcating from another simple eigenvalue $d_{1,2} = 1.98$, with the resulting spatial modes exhibiting higher amplitudes.

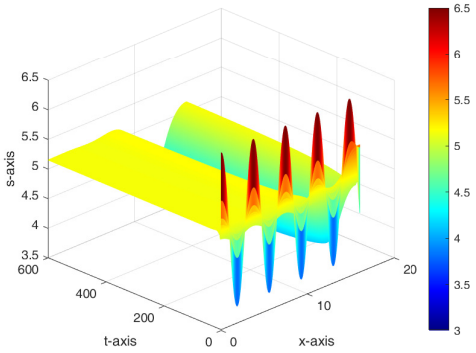

(a) A $3D$ view of the concentration of biomass s.

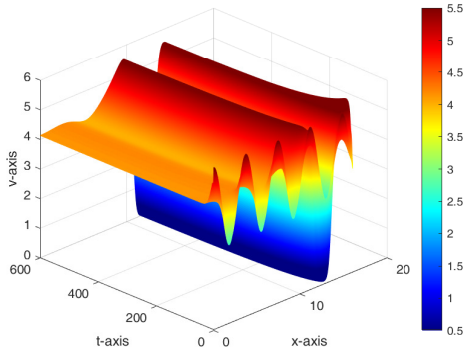

(b) A $3D$ view of the concentration of biomass v.

Figure 4. Steady-state bifurcation solution at the simple eigenvalue for $d_1 = 6.56, d_2 = 0.1, h = 3.33, v_m = 10, p = 2.12$, and $c = 1.11$. The bifurcation direction is subcritical.

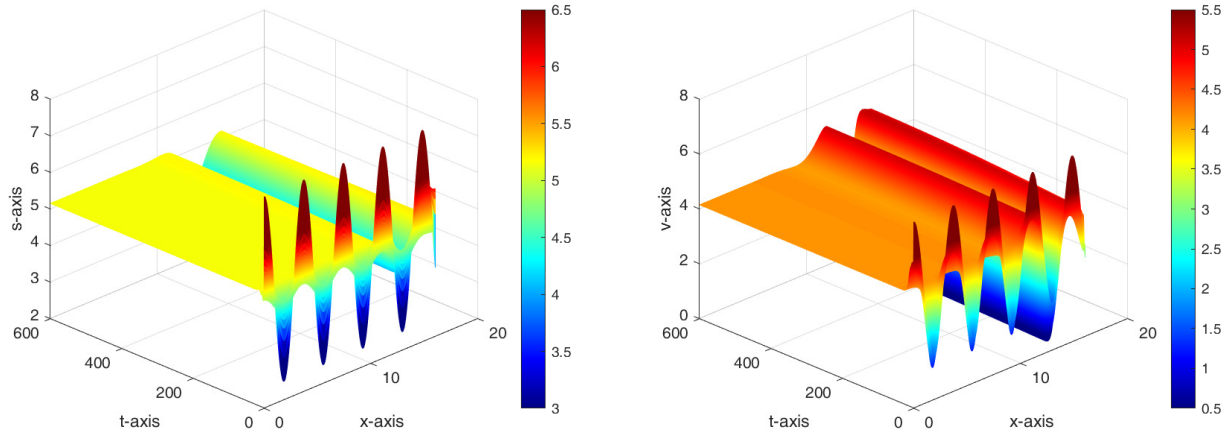

(a) A 3D view of the concentration of biomass s.

(b) A 3D view of the concentration of biomass v.

Figure 5. Steady-state bifurcation solution at the simple eigenvalue for $d_1 = 1.98, d_2 = 0.1, h = 3.33, v_m = 10, p = 2.12$, and $c = 1.11$. The bifurcation direction is subcritical.

By letting $d_2 = 0.02$, we obtain $d_{1,1} = d_{1,2} = \tilde{d}_1 = 7.98$, and $(s_0, v_0) = (5.15 + 0.1\cos(1.7x),\ 4.15 + 0.1\cos(1.7x))$. By Theorem 4.1(ii), a double bifurcation point $(\tilde{d}_1, (s_*, v_*))$ is shown in Figure 3(b), and a steady-state bifurcation occurs at $d_1 = \tilde{d}_1 = 7.98$, as illustrated in Figure 6, where the spatial modulation pattern is visibly smoother and nearly sinusoidal, with a smaller amplitude compared to Figures 4 and 5.

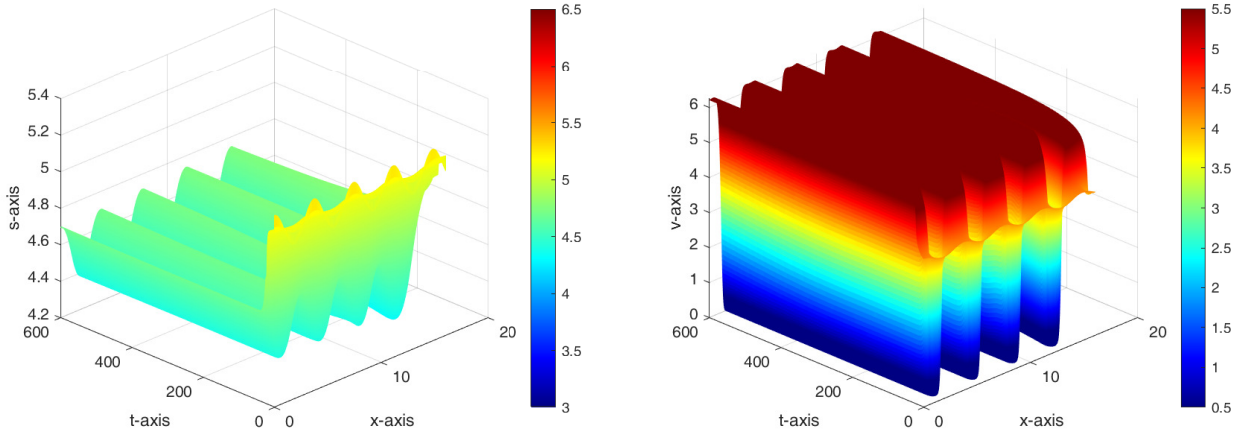

(a) A 3D view of the concentration of biomass s.

(b) A 3D view of the concentration of biomass v.

Figure 6. Steady-state bifurcation solution at the double eigenvalue for $d_1 = 7.98, d_2 = 0.02, h = 3.33, v_m = 10, p = 2.12$, and $c = 1.11$.

If d_1, d_2, h, v_m, p, and c are chosen suitably, system (1.4) can generate periodic solutions. By choosing $d_1 = 0.01, d_2 = 0.42, h = 3.33, v_m = 10, p = 2.82, c = 1.11$, and $(s_0, v_0) = (3.14 + 1.34\cos 1.7x, 2.14 + 1.34\cos 1.7x)$, spatially homogeneous periodic solutions of

system (1.4) can occur as shown in Figure 7. Figure 7(a),(b) present the 3D evolution of biomass s and v, and Figure 7(c),(d) illustrate their time evolution at representative spatial locations.

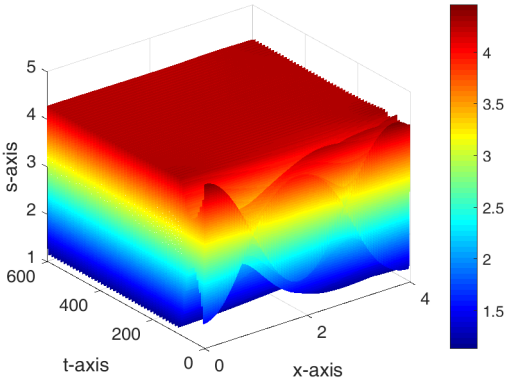

(a) A 3D view of the concentration of biomass s.

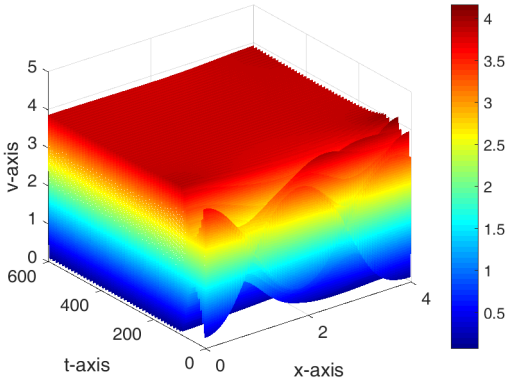

(b) A 3D view of the concentration of biomass v.

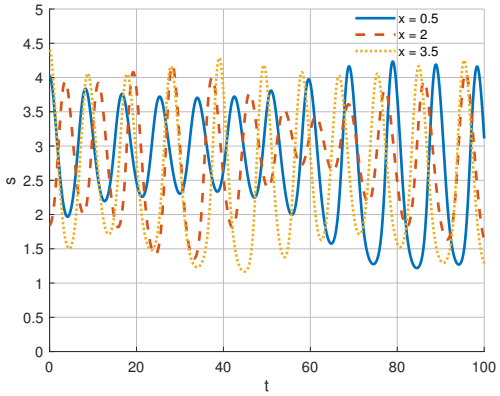

(c) Time evolution.

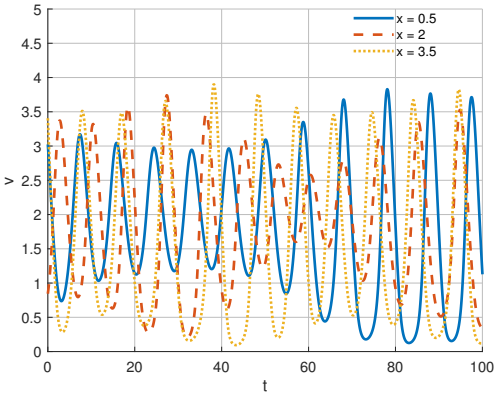

(d) Time evolution.

Figure 7. Numerical simulation of spatially homogeneous and stable periodic solutions to system (1.4) for $d_1 = 0.01$, $d_2 = 0.04$, $h = 3.33$, $v_m = 10$, $p = 2.82$, and $c = 1.11$.

5.3. Pattern formation

For the parameter set $d_1 = 1$, $d_2 = 0.01$, $c = 3$, $p = 3.8$, and $v_m = 4$, Figures 8 and 9 illustrate the evolution of vegetation patterns for $h = 2.78$ and $h = 2.6$, respectively. In Figure 8, as t increases, the patterns stabilize with strips gradually disappearing while spots persist. In contrast, Figure 9 shows that with further increase in t, both strip and spot patterns coexist throughout the domain. Here, the blue region indicates bare soil, whereas the red region denotes areas of high vegetation concentration.

For the parameter set $d_1 = 1$, $d_2 = 0.01$, $v_m = 4$, and $c = 3$, the evolution of vegetation patterns under varying intrinsic growth rate h and sand burial rate p in a two-dimensional domain is illustrated in Figure 10 for $p = 3.8$ and Figure 11 for $h = 2.78$. As the patterns stabilize, a gradual reduction in h combined with an increase in p leads to the progressive disappearance of strips, eventually forming rings and markedly lowering vegetation density.

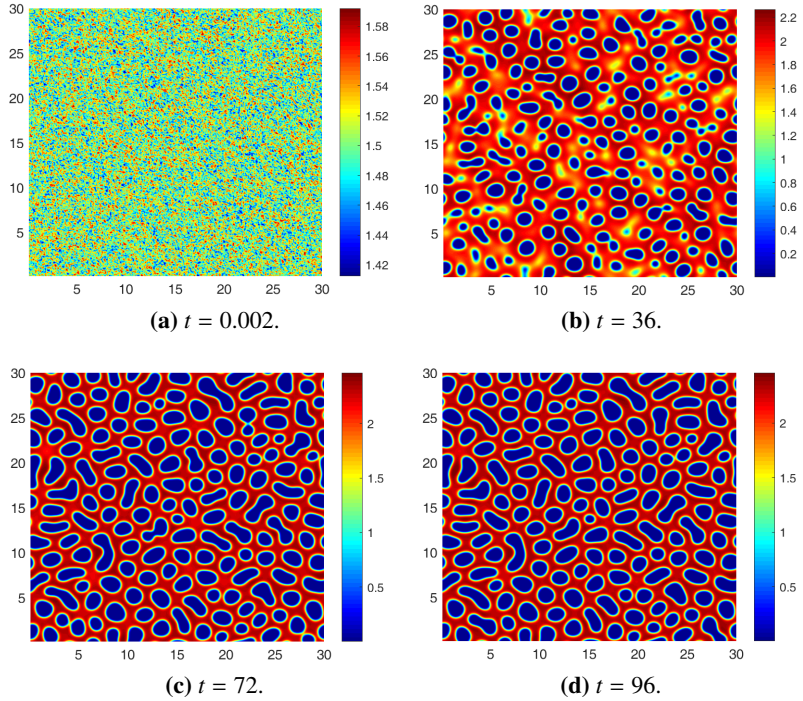

(a) $t = 0.002$. **(b)** $t = 36$.

(c) $t = 72$. **(d)** $t = 96$.

Figure 8. Plant pattern formation governed by (1.4) with $d_1 = 1$, $d_2 = 0.01$, $v_m = 4$, $p = 3.8$, $c = 3$, and $h = 2.78$.

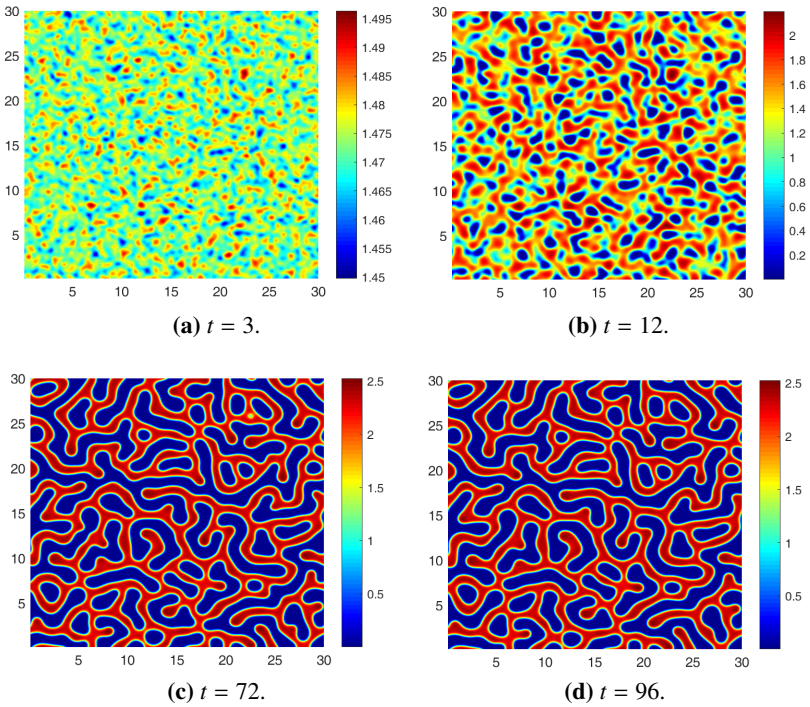

(a) $t = 3$. **(b)** $t = 12$.

(c) $t = 72$. **(d)** $t = 96$.

Figure 9. Pattern formation in plant distribution governed by (1.4), where $d_1 = 1$, $d_2 = 0.01$, $v_m = 4$, $p = 3.8$, $c = 3$, and $h = 2.6$.

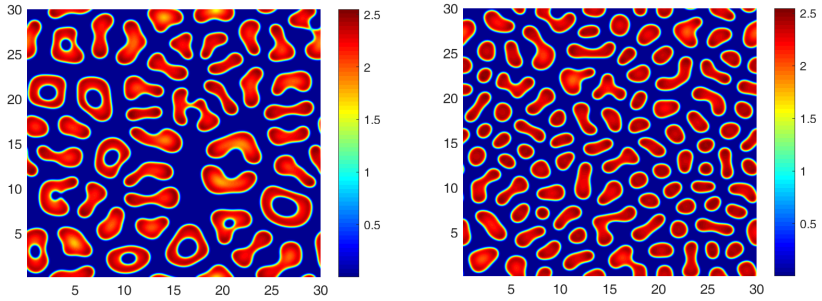

(a) $h = 2.52$. **(b)** $h = 2.53$.

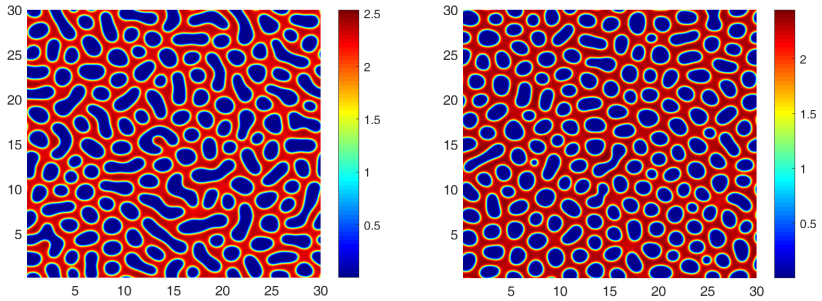

(c) $h = 2.7$. **(d)** $h = 2.8$.

Figure 10. Patterned plant distribution in (1.4) with $d_1 = 1, d_2 = 0.01, v_m = 4, p = 3.8$, and $c = 3$.

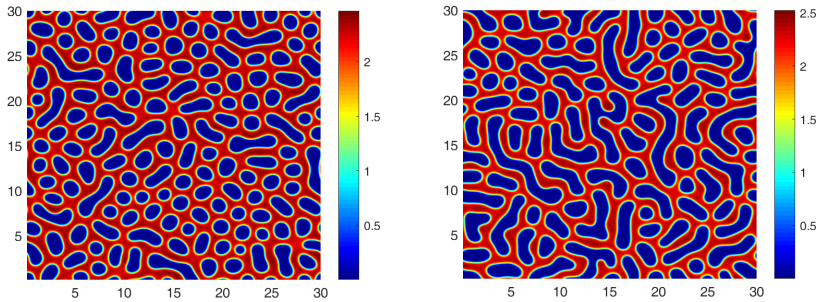

(a) $p = 3.84$. **(b)** $p = 4$.

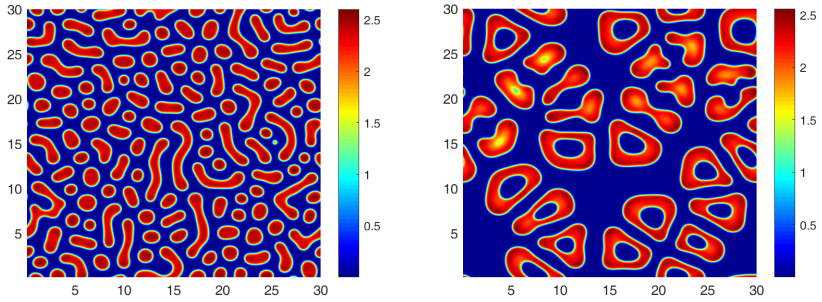

(c) $p = 4.1$. **(d)** $p = 4.15$.

Figure 11. Patterned plant distribution in (1.4) with $d_1 = 1, d_2 = 0.01, v_m = 4, h = 2.78$, and $c = 3$.

6. Conclusions

To investigate the ecological mechanisms underlying aeolian sand vegetation pattern formation, enhance the representation of vegetation competition across ecosystems, and improve insights into desertification and restoration, we examine the spatial-temporal complexity of vegetation dynamics in arid and semi-arid regions, with an emphasis on vegetation system modeling and theoretical analysis. A diffusive vegetation-sand model subject to Neumann boundary conditions is investigated. Linear stability analysis identifies the parameter regime where Turing instability may arise. Using the maximum principle, a priori estimates for positive steady-state solutions are derived. Steady-state bifurcations associated with both simple and double eigenvalues are then examined separately. The global bifurcation structure originating from simple eigenvalues is constructed, and sufficient conditions for determining the bifurcation direction are obtained. In the case of double eigenvalues, techniques such as space decomposition and the implicit function theorem are employed. Finally, numerical simulations are conducted to verify and enhance the theoretical findings.

The types of vegetation-sand patterns are diverse, and the formation mechanisms are complex. The characteristics of these patterns and their variations with environmental parameters and human activities demonstrate the complexity of vegetation patterns. We consider a type of vegetation-sand model with diffusion and conduct a preliminary exploration of the formation, characteristics, and stability of wind-vegetation patterns. However, there are many questions that need further research to be resolved, such as, adding the advection term by the prevailing wind in the model to explore more complex vegetation-sand models. Alternatively, by discretizing the continuous vegetation-sand model, one may employ discrete event systems to characterize the dynamics of sand particles and vegetation, including sand transport and its impact frequency. Discrete modeling is particularly suitable for capturing sand deposition and vegetation discontinuities.

Use of AI tools declaration

The authors declare they have not used Artificial Intelligence (AI) tools in the creation of this article.

Acknowledgments

This work is supported by the National Natural Science Foundation of China (No. 61872227).

Conflict of interest

The authors declare there is no conflict of interest.

References

1. F. Zhang, Y. Li, Y. Zhao, Z. Liu, Vegetation pattern formation and transition caused by cross-diffusion in a modified vegetation-sand model, *Int. J. Bifurcation Chaos*, **32** (2022), 2250069. https://doi.org/10.1142/S0218127422500699
2. L. P. White, Vegetation stripes on sheet wash surfaces, *J. Ecol.*, **59** (1971), 615–622. https://doi.org/10.2307/2258335

3. L. P. White, Vegetation arcs in Jordan, *J. Ecol.*, **57** (1969), 461–464. https://doi.org/10.2307/2258392
4. Y. Toda, Y. Zhou, N. Sakai, Modeling of riparian vegetation dynamics and its application to sand-bed river, *J. Hydro-environ. Res.*, **30** (2020), 3–13. https://doi.org/10.1016/j.jher.2019.09.003
5. F. Zhang, H. Zhang, T. Huang, T. Meng, S. Ma, Coupled effects of Turing and Neimark-Sacker bifurcations on vegetation pattern self-organization in a discrete vegetation-sand model, *Entropy*, **19** (2017), 478. https://doi.org/10.3390/e19090478
6. M. C. M. de M. Luna, E. J. R. Parteli, O. Durán, H. J. Herrmann, Model for the genesis of coastal dune fields with vegetation, *Geomorphology*, **129** (2011), 215–224. https://doi.org/10.1016/j.geomorph.2011.01.024
7. G. Sun, H. Zhang, Y. Song, L. Li, Z. Jin, Dynamic analysis of a plant-water model with spatial diffusion, *J. Differ. Equations*, **329** (2022), 395–430. https://doi.org/10.1016/j.jde.2022.05.009
8. G. Guo, Q. Qin, D. Pang, Y. Su, Positive steady-state solutions for a vegetation-water model with saturated water absorption, *Commun. Nonlinear Sci. Numer. Simul.*, **131** (2024), 107802. https://doi.org/10.1016/j.cnsns.2023.107802
9. G. Gan, Y. Liu, G. Sun, Understanding interactions among climate, water, and vegetation with the Budyko framework, *Earth Sci. Rev.*, **212** (2021), 103451. https://doi.org/10.1016/j.earscirev.2020.103451
10. P. Carter, A. Doelman, A. Iuorio, F. Veerman, Travelling pulses on three spatial scales in a Klausmeier-type vegetation-autotoxicity model, *Nonlinearity*, **37** (2024), 095008. https://doi.org/10.1088/1361-6544/ad6112
11. M. Abbas, F. Giannino, A. Iuorio, Z. Ahmad, F. Calabrò, PDE models for vegetation biomass and autotoxicity, *Math. Comput. Simul.*, **228** (2025), 386–401. https://doi.org/10.1016/j.matcom.2024.07.004
12. C. A. Klausmeier, Regular and irregular patterns in semiarid vegetation, *Science*, **284** (1999), 1826–1828. https://doi.org/10.1126/science.284.5421.1826
13. S. van der Stelt, A. Doelman, G. Hek, J. D. M. Rademacher, Rise and fall of periodic patterns for a generalized Klausmeier-Gray-Scott model, *J. Nonlinear Sci.*, **23** (2013), 39–95. https://doi.org/10.1007/s00332-012-9139-0
14. E. Meron, J. J. R. Bennett, C. Fernandez-Oto, O. Tzuk, Y. R. Zelnik, G. Grafi, Continuum modeling of discrete plant communities: Why does it work and why is it advantageous? *Mathematics*, **7** (2019), 987. https://doi.org/10.3390/math7100987
15. E. Meron, E. Gilad, J. von Hardenberg, M. Shachak, Y. Zarmi, Vegetation patterns along a rainfall gradient, *Chaos Solitons Fractals*, **19** (2004), 367–376. https://doi.org/10.1016/S0960-0779(03)00049-3
16. E. Meron, Vegetation pattern formation: The mechanisms behind the forms, *Phys. Today*, **72** (2019), 30–36. https://doi.org/10.1063/PT.3.4340
17. G. Guo, J. You, K. A. Abbakar, Pattern dynamics in a water-vegetation model with cross-diffusion and nonlocal delay, *Math. Methods Appl. Sci.*, **48** (2025), 3190–3213. https://doi.org/10.1002/mma.10480

18. F. Zhang, H. Zhang, M. R. Evans, T. Huang, Vegetation patterns generated by a wind driven sand-vegetation system in arid and semi-arid areas, *Ecol. Complexity*, **31** (2017), 21–33. https://doi.org/10.1016/j.ecocom.2017.02.005

19. Y. Maimaiti, Z. Lv, A. Muhammadhaji, W. Zhang, Analyzing vegetation pattern formation through a time-ordered fractional vegetation-sand model: A spatiotemporal dynamic approach, *Networks Heterogen. Media*, **19** (2024), 1286–1308. https://doi.org/10.3934/nhm.2024055

20. F. Zhang, L. Yao, W. Zhou, Q. You, H. Zhang, Using shannon entropy and contagion index to interpret pattern self-organization in a dynamic vegetation-sand model, *IEEE Access*, **8** (2020), 17221–17230. https://doi.org/10.1109/ACCESS.2020.2968242

21. H. Zhang, Y. Wu, G. Sun, C. Liu, G. Feng, Bifurcation analysis of a spatial vegetation model, *Appl. Math. Comput.*, **434** (2022), 127459. https://doi.org/10.1016/j.amc.2022.127459

22. X. Wang, J. Shi, G. Zhang, Bifurcation and pattern formation in diffusive Klausmeier-Gray-Scott model of water-plant interaction, *J. Math. Anal. Appl.*, **497** (2021), 124860. https://doi.org/10.1016/j.jmaa.2020.124860

23. G. Guo, J. Wang, Pattern formation and qualitative analysis for a vegetation-water model with diffusion, *Nonlinear Anal.:Real World Appl.*, **76** (2024), 104008. https://doi.org/10.1016/j.nonrwa.2023.104008

24. X. Wang, W. Wang, G. Zhang, Vegetation pattern formation of a water-biomass model, *Commun. Nonlinear Sci. Numer. Simul.*, **42** (2017), 571–584. https://doi.org/10.1016/j.cnsns.2016.06.008

25. G. Grifó, G. Consolo, C. Curró, G. Valenti, Rhombic and hexagonal pattern formation in 2D hyperbolic reaction-transport systems in the context of dryland ecology, *Phys. D Nonlinear Phenom.*, **449** (2023), 133745. https://doi.org/10.1016/j.physd.2023.133745

26. J. Wu, G. S. K. Wolkowicz, A system of resource-based growth models with two resources in the unstirred chemostat, *J. Differ. Equation*, **172** (2001), 300–332. https://doi.org/10.1006/jdeq.2000.3870

27. J. Wu, H. Nie, G. S. K. Wolkowicz, A mathematical model of competition for two essential resources in the unstirred chemostat, *SIAM J. Appl. Math.*, **65** (2004), 209–229. https://doi.org/10.1137/S0036139903423285

28. Y. Ma, R. Yang, Bifurcation analysis in a modified Leslie-Gower with nonlocal competition and Beddington-DeAngelis functional response, *J. Appl. Anal. Comput.*, **15** (2025), 2152–2184. https://doi.org/10.11948/20240415

29. F. Zhu, R. Yang, Bifurcation in a modified Leslie-Gower model with nonlocal competition and fear effect, *Discrete Contin. Dyn. Syst.-Ser. B*, **30** (2025), 2865–2893. https://doi.org/10.3934/dcdsb.2024195

30. Y. Lou, W. Ni, Diffusion, self-diffusion and cross-diffusion, *J. Differ. Equations*, **131** (1996), 79–131. https://doi.org/10.1006/jdeq.1996.0157

31. M. G. Crandall, P. H. Rabinowitz, Bifurcation from simple eigenvalues, *J. Funct. Anal.*, **8** (1971), 321–340. https://doi.org/10.1016/0022-1236(71)90015-2

32. P. H. Rabinowitz, Some global results for nonlinear eigenvalue problems, *J. Funct. Anal.*, **7** (1971), 487–513. https://doi.org/10.1016/0022-1236(71)90030-9

33. Y. Nishiura, Global structure of bifurcating solutions of some reaction-diffusion systems, *SIAM J. Math. Anal.*, **13** (1982), 555–593. https://doi.org/10.1137/0513037

34. I. Takagi, Point-condensation for a reaction-diffusion system, *J. Differ. Equations*, **61** (1986), 208–249. https://doi.org/10.1016/0022-0396(86)90119-1

35. J. Shi, Persistence and bifurcation of degenerate solutions, *J. Funct. Anal.*, **169** (1999), 494–531. https://doi.org/10.1006/jfan.1999.3483

AIMS Press